ELT - MICADO

Phase B

Primary Science Case

Doc. No.: ELT-TRE-MCD-563XX-YYYY

Issue: 1.0

Date: dd.mm.yyyy

Author(s): E. Tolstoy...

Name Date Signature

R. Davies...

Name Date Signature

WP Manager: E. Tolstoy...

Name Date Signature

Proj. Responsible R. Davies...

Name Date Signature

CHANGE RECORD

ISSUE	DATE	SECTION/PARAGRAPH AFFECTED	REASON/INITIATION DOCUMENTS/REMARKS
1.0	dd.mm.yyyy	All	Initial issue

TABLE OF CONTENTS

Scope

This document describes the set of science cases developed for MICADO operating on the E-ELT. It builds on and updates the Phase A science case. There are cases for both SCAO and MCAO imaging modes as well as MCAO spectroscopy. This is not a document to set out the GTO priorities. The aim is to cover a wide range of possible science cases and ensure that the capabilities of the instrument and telescope are and remain sufficient to carry out these studies.

References

Applicable documents

RD Nr	Doc. Nr	Doc .Title	Issue	Date
UCD	ELT-PLA-MCD-56301-0002	Science Use Cases	x.y	dd.mm.yyyy

Reference documents

The following reference documents (RD) contain useful information relevant to the subject of the present document.

RD Nr	Doc. Nr	Doc .Title	Issue	Date
RD1		Operational Concept Description		dd.mm.yyyy

Table 1: Reference documents

Acronyms

AD	Applicable Document
ANF	Antofagasta
AOWFC	Adaptive Optics Wave-Front-sensor Camera
CAD	Computer-Aided Design
CIDL	Configuration Item Data List
CMMS	Computerized Maintenance Management System
Co-Pi	Co-Principal Investigator
CPL	Common Pipeline Library
CRE	Change Request
DD	Deliverable Document
DFS	Data Flow System
DICB	Data Interface Control Board
DRD	Document Requirements Definition
E-ELT	European Extremely Large Telescope
EMC	Electromagnetic Compatibility
ESO	European Southern Observatory
ETC	Exposure Time Calculator
FEA	Finite Element Analysis
FMECA	Failure Mode Effect and Criticality Analysis
FDR	Final Design Review
GTO	Guaranteed Time Observations
HDRL	High Level Data Reduction library
ICD	Interface Control Document
ICS	Instrument Control Software
IRM	Integration Readiness Meeting
KM	Key Milestone
KOM	Kick Off Meeting
LPO	La Silla Paranal Observatory
LRU	Line Replacement Unit
M4	4^{th} mirror in E-ELT
M5	5^{th} mirror in E-ELT
MAIT	Manufacturing Assembly Integration and Test

MAORY	Multi-conjugate Adaptive Optics RelaY
MCAO	Multi-conjugate Adaptive Optics
MICADO	Multi-AO Imaging Camera for Deep Observations
MTBF	Mean Time Between Failure
OCD	Operations Concept Description
PAE	Preliminary Acceptance Europe
PA	Product Assurance
PAC	Provisional Acceptance Chile
PDR	Preliminary Design Review
PI	Principal Investigator
POA	Paranal or Armazones
RAM	Reliability Availability Maintainability
RD	Reference Document
RFW	Request for Waiver
RTC	Real-Time Computer
QA	Quality Assurance
SCAO	Single-conjugate Adaptive Optics
SCL	Santiago de Chile
SOW	Statement of Work
SV	Science Verification
TBC	To Be Confirmed
TBD	To Be Defined
TCS	Telescope Control Software
TRL	Technology Readiness Level
TRM	Test Readiness Meeting
TS	Technical Specification
VLT	Very Large Telescope
WBS	Work Breakdown Structure
WFRTC	Wave-Front Real-Time Computer
WP	Work Package

1. MICADO science capabilities

MICADO is designed to work between 0.8-2.5microns, and with the assistance of a single or multi-conjugate adaptive optics system, provided by MAORY, at the diffraction limit of the E-ELT. The primary mode is imaging, with an emphasis on astrometry. In the MCAO mode there is a wide field option, where the field of view will be ~50arcsec square with a pixel scale of 4mas. There is also a zoom mode with a finer 1.5mas pixel scale over ~20arcsec field of view. MICADO images will provide comparable sensitivity to JWST (James Webb Space Telescope) at 6 times better spatial resolution, and enable proper motions as small as 5km/s to be measured at distances of up to 100kpc. High contrast imaging using a coronagraph will allow high precision differential imaging. MICADO also includes a long-slit spectroscopic mode that is optimised for compact objects, with extended wavelength coverage at moderate resolution. High time resolution imaging is also possible. These capabilities make a wide range of break-though science cases feasible.

The superior angular resolution of MICADO images makes crowded field photometry and astrometric applications especially attractive. Exciting opportunities include mapping individual stellar orbits in external stellar systems and monitoring flaring gas fainter and closer to the event horizon of the central black hole in the Galaxy than ever before. Astrometry can also be extended to monitor black holes in other galaxies, and the central regions of globular clusters. Trigonometric parallaxes and proper motions of numerous individual stars in resolved stellar systems will allow a more active view of how stellar systems move and change. This will, amongst many other things, enable us to trace the presence (or absence) of black holes in a range of environments, as well as making accurate mass models by combining these results with radial velocity measurements to obtain a 3D view of stellar motions. We will be able to map the dark matter distribution in a variety of environments and for a range of spatial and temporal scales, and potentially set constraints on the physical nature of dark matter particles.

Galaxy formation and evolution will always remain a central theme in observational astrophysics, and with the spatial resolution of MICADO it will be possible to make uniquely detailed studies of both local and very high redshift galaxies, and everything in between. In the nearby Universe, where individual stars can be resolved, star formation histories using optical/IR colour-magnitude diagrams, will be possible well within the main body of dense stellar systems in the dense regions of nearby spiral galaxies in nearby galaxy groups all the way out to the nearest of galaxy clusters (e.g., Virgo, Fornax). This will be possible for a wide variety of galaxy masses, and types, from very small dwarf galaxies to the most massive Elliptical galaxies, in a range of different environments. A critical question that this will allow us to answer is: how representative are the Milky Way and M31 of galaxy formation and evolution processes everywhere in the Universe? For much more distant, intermediate and high redshift galaxies multi-wavelength broad-band and narrow-band imaging will reveal the structure of galaxies at the peak of their star formation activity, mass assembly, and morphological transformations. MICADO will also be able to probe the star formation activity in the centres of dense active galaxies in extraordinary detail, to trace the evolution with redshift of the black hole mass and determine how this relates to the other galaxy properties, such as the bulge properties. This relates to the detailed effects of AGN feedback, and the role of environment in triggering and shutting down activity.

MICADO will also study of the solar system as well as exo-planets, distant planetary systems over a range of evolutionary stages to probe the initial conditions for planetary formation and the evolution of planetary systems over various time-frames. Until the arrival of the extreme-AO instrument on E-ELT MICADO will provide the most detailed view of planetary systems that are not highly shrouded in dust.

This document gives an overview of the details of the main science cases for MICADO.

2. The Galactic Centre

Text taken from Phase A study. Needs updating - taking account of GRAVITY; new figs?
ET edited text a bit. 20/9/16
Coordinator: Ric Davies/MPE Stefan Gillessen
Technical Templates: A.1 (imaging), A.2 (spectroscopy)

2.1 Background Information

The Centre of the Milky Way is a unique laboratory for exploring strong gravity around the closest massive black hole (MBH), and for studying fundamental and broadly relevant processes happening in the very dense star cluster surrounding this MBH, at a level of detail and quality that will not ever be possible in external galaxies (see Figure 2.1). The Galactic Centre also serves as a crucial guide for theoretical studies of accretion onto MBHs and the important issue of co-evolution of MBH activity and nuclear star formation.

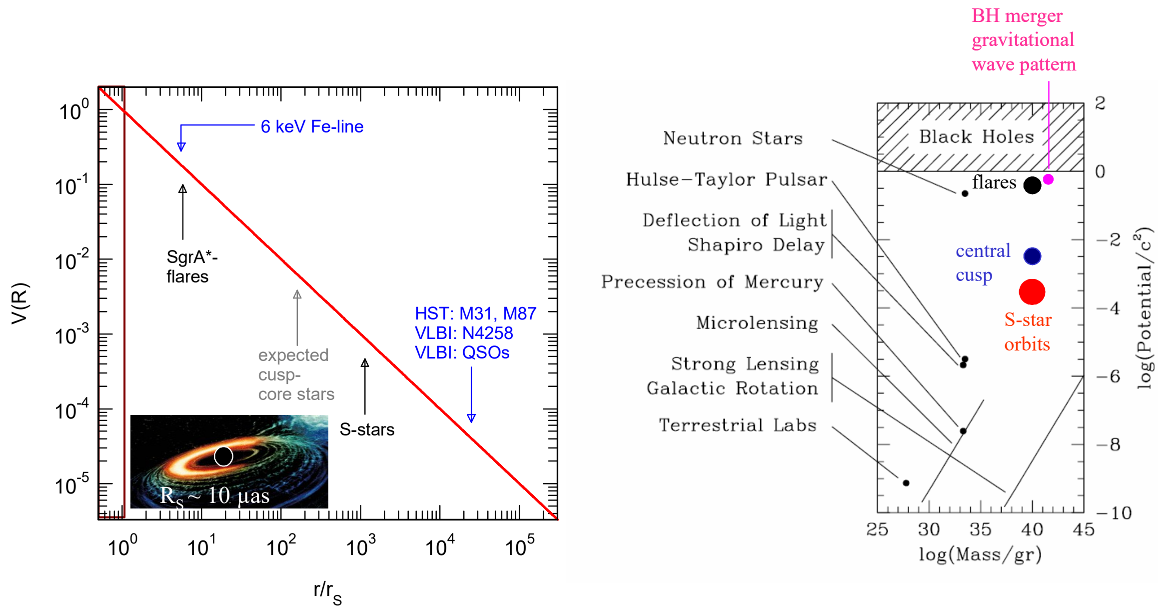

Figure 2.1 left: Gravitational Potential around a (massive) black hole, as a function of radius in units of the radius of the event horizon. Current dynamical measurements in the Galactic Centre ('S-stars') probe to ~1000 R_s, while external galaxies (blue) probe to ~3x10^4 R_s. Measurements with MICADO/EELT will probe faint cusp stars ten times further to the event horizon, where $\square^2$-effects of Special and General Relativity, as well as the Schwarzschild precession term can be observed. GRAVITY-VLTI observations of infrared flares and potentially also spectrally resolved X-ray reverberation mapping of the 6.4 keV Fe-line may be able to push dynamical measurements into the very strong curvature regime at a few times R_s. Right: comparison of different probes of gravity, as a function of mass scale (horizontal) and field curvature (vertical). The Galactic Centre stellar orbits and flares probe a hitherto totally untested regime of mass and field curvature.

Arguably the most fundamental goal of Galactic Centre research in the next decades will be dynamical measurements of the gravitational potential ever closer to the event horizon, with the ultimate goal of testing General Relativity in the strong field limit. The currently available observations with the VLT and Keck of the orbits of ~ 30 bright 'S-stars' in the stellar cusp around the MBH coincident with the compact radio source SgrA* provide the best tool available in astrophysics today for clean dynamical measurements of the gravitational potential to a scale of ≥10^3 times the radius of the event horizon, R_s (left panel of Figure 2.1). The best observations in external galaxies can sample >3×10^4 R_s. The VLT/Keck observations are strongly limited by confusion. Fainter stars than presently observable are very likely present, as the observed K-band luminosity function (KLF) is very steep (see Figure 2.2). The volume density of the S-stars increases inward with $R^{-1.3\pm0.1}$, such that it is likely that higher resolution measurements will find fainter stars at 10^2-10^3 R_s. At that radius, orbital velocities approach 0.1c and orbital periods may be as short as a few years, allowing the detection of the effects of Special and General Relativity (SR and GR) on these orbits. Such measurements will test SR and GR in a hitherto completely unexplored regime of field curvature and mass scale (right panel of Figure 2.1). Still further in, at a radius of a few R_s, variable infrared emission from transiently accelerated electrons ('flares') probe the innermost accretion zone around the MBH. Detection of orbital motions of this hot gas requires an astrometric precision of about 10 micro-arcseconds on time scales of a few hours.

Because of the effects of confusion, the current precision of astrometric measurements is significantly worse than the fundamental measurement limit. Higher resolution observations (with higher precision and lower confusion) are required to detect the Newtonian precession of these orbits due to any extended mass outside of the central MBH. Such a mass distribution consists of the observed stars themselves (<10^2 $M_\odot$ in the central 0.1") and in addition, stellar remnants (stellar BHs and neutron stars: estimated to be ≤10^4 $M_\odot$) and perhaps dark matter. Detection of these components is obviously of great interest, also for determining the expected rates of extreme mass ratio inspiral events leading to gravitational waves.

Figure 2.1: Observed K-band luminosity function (KLF) of the central 0.8", as observed with NACO on the VLT (solid blue line), compared to a t=10^7 yr age population with a Salpeter IMF (dotted black line). Combined with the observed $R^{-1.3+/-0.1}$ power law, stellar density distribution, this means that there are likely to be ~5-10 K<20 stars in the central 0.1-0.2".

Another important issue is whether the gas that falls into the nuclear region forms stars near the MBH, or whether it is accreted directly into the MBH, and whether nuclear star formation and MBH activity are related. Current observations of the Galactic Centre have yielded the remarkable result that episodic star formation deep in the sphere of influence of the MBH appears to be efficient, and apparently has a top-heavy mass function. A better quantitative determination of the processes involved in stellar formation in this extreme environment, a precise determination of the resulting stellar mass function and the exploration of the connection between the rates of star formation and black hole accretion are critical for understanding the cosmological co-evolution of galaxies and MBHs.

Finally the Galactic Centre MBH (SgrA*) is the prototype of the very common class of highly radiatively inefficient accretion sources (L/L_{edd}~10^{-8} − 10^{-6}). Detailed multi-wavelength observations of SgrA* are beginning to shed light on the complex physics underlying this inefficient accretion process that appears to dominate at relatively low accretion rates and is guiding current theoretical work. Future work will emphasize high time resolution, spectrally resolved observations and polarization studies. Astrometry of the ‘infrared’ flares will be extremely exciting but probably requires ~10µarcsecond resolution.

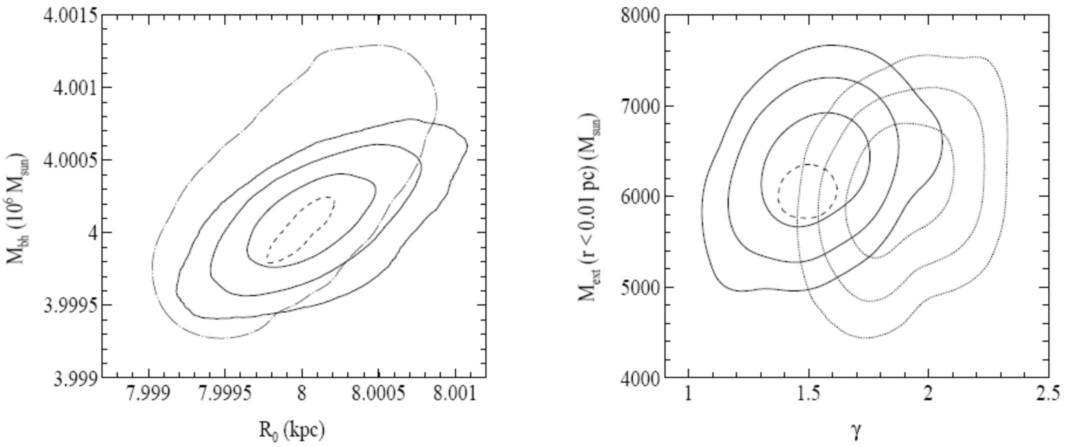

Figure 2.2: Examples of the precision of parameter estimations in the Galactic Centre, obtained from simulations of stellar orbital astrometric and radial velocity data with an ELT (taken from the TMT study by Weinberg, Milosavljevic & Ghez 2005), Left: 1, 2 and 3□ uncertainty contours (solid) of mass and distance to the Galactic Centre MBH obtained from an astrometric study of 20 stars with a modest precision of 500µarcsec and 10 km/s. The dotted contour gives the 3□ contour for a 5 times higher precision, which will be achievable with MICADO. Right: Same for the estimate of the extended mass around the MBH for two different choices of the power law slope γ of the cusp’s density distribution.

2.2 Importance of MICADO

MICADO is uniquely suited for the exploration of the Galactic Centre. The central stellar cusp around SgrA* is strongly confusion limited for current AO observations on 8m class telescopes, limiting the reliable detection and measurement of position of stars to K~16-17.5, which corresponds to main sequence B-stars. The combination of MICADO and the EELT will push the effective stellar detection sensitivity by ≥5 magnitudes in modest integration times, making studies of even subsolar mass stars possible and allowing mass function studies across the entire range of stellar masses. It should be possible to carry out astrometry with a long term precision of 50-100 µarcsec with MICADO, this is 3 to 6 times better than currently with NACO at the VLT. At that level of precision a number of key issues of the physics of massive black holes and their surroundings can be tackled. MICADO research on the Galactic Centre will likely concentrate on the following issues:

- detection of β^2 (β=v/c) post-Newtonian effects of SR and GR, as well as possibly the Schwarzschild pro-grade precession term, for some of the orbits of the already known S-stars to K~17.5, in particular the stars S2 and S14, which have the smallest peri-bothroi (15-20 light hours). Because of the confusion with fainter stars these effects will almost certainly not be measurable in proper motion data with current 8m-class telescopes, even with great patience;
- detection of the theoretically predicted cusp of stellar remnants (stellar black holes and neutron stars) by the Newtonian retro-grade precession of the apo-bothroi of the known S-

stars. Of special interest is the possible detection of more massive intermediate mass black holes that have been hypothesized to form in dense star clusters outside the Galactic Centre and then secularly sink into the central cusp by dynamical friction. The determination of this dark cusp is of great general importance for predicting event rates for LISA large mass ratio in-spiral events. Simulations show that MICADO will be able to determine the mass of this extended dark halo around the MBH with an accuracy of less than a few per cent (Fehler: Referenz nicht gefunden);

- determination of the orbits of fainter (K≤20-21) main sequence stars in the inner cusp, with semi-major axes significantly smaller than the current S-stars, using both astrometric data and Doppler spectroscopy. Extrapolations from the surface density distribution and KLF indicate ~5-10 stars with K≤20 (m≥1.4 M$_\odot$) in the innermost 0.1-0.2”, of which a few stars may have peri-bothroi <10^3 R$_s$, several times smaller than that of S2. Such stars would have orbital time scales of a few years. In this case the Schwarzschild precession term and other GR terms will be detectable in a decade of observations (Figure 2.4).

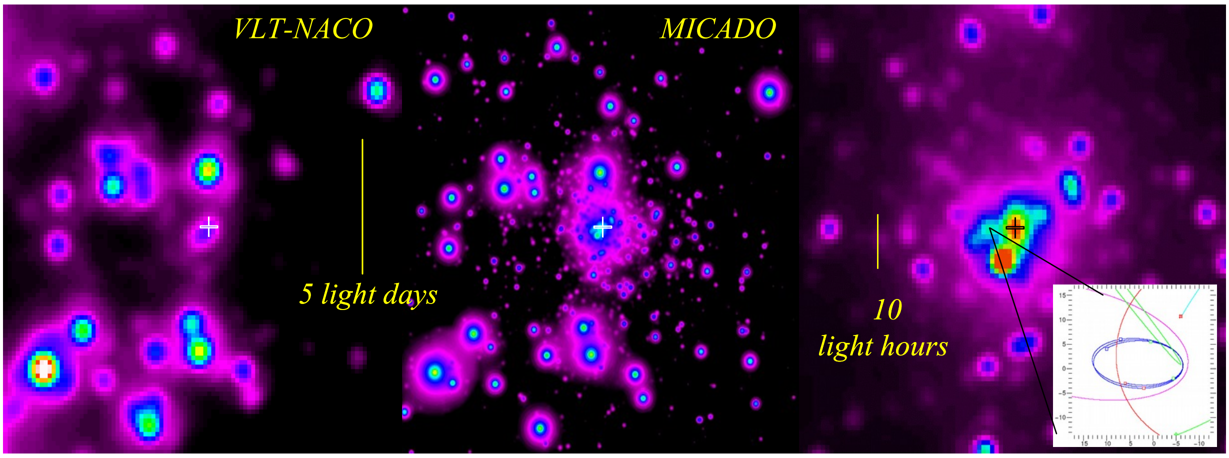

Figure 2.3: A simulation of a MICADO image of the central cusp around the MBH in the Galactic centre, compared to a current high-quality VLT/NACO K-image at 60 mas resolution (left). The KLF- and surface density information and extrapolating NCAO results to fainter magnitudes with a Salpeter IMF yields the simulated MICADO image in the central panel (on the same scale as the NACO image). The rightmost panel shows a zoom into the central region of the MICADO image. A number of stars in this image are close enough to the central MBH (cross) that the Schwarzschild precession of their orbits should be observable for sufficiently high ellipticity, as depicted in the simulation in the lower right corner.

- Study of the central accretion zone surrounding SgrA*. With the resolution of the EELT (5-10 mas) it will possible to study in detail the spectral and temporal properties of accretion events and search for evidence of outflows/jets predicted for radiatively inefficient accretion flows as in the Galactic Centre. Short term astrometry within an accretion event, as well as the search for positional shifts between accretion events at different times are of great interest for finding evidence for orbital motion and outflow of the hot gas and the predicted Brownian motion of the central massive black hole;
- with the outstanding astrometric precision of the EELT (50-100µarcsec) it will be possible to determine orbits of ~10^3 individual stars over a decade of observation. From such data it will be possible to determine the distance to the Galactic Centre to 0.1-0.3%, thus enabling a number of powerful constraints on the dynamics of the Galaxy (Fehler: Referenz nicht gefunden). It will also be possible to explore stellar phase space clumping directly (such as the one or two disks of young massive stars already known), binary fractions and to search for possible intermediate mass black holes in the central cluster;
- outside of the central parsec, EELT astrometry will allow dynamical measurements of the other prominent young star clusters in the central 50pc (Arches, Quintuplet etc.). Perhaps the most intriguing issue is the search for possible intermediate mass black holes there (as in globular clusters). The unambiguous detection of an intermediate mass black hole in such a cluster has far-reaching consequences for seed black hole formation during the epoch of reionisation;
- with the high angular resolution and enormous sensitivity of the EELT & MICADO it will be possible to count stars to <1 $M_\odot$ and establish the present day mass function. In combination with colours and spectra it will then be possible to determine a robust initial mass function in the Galactic Centre and test the emerging evidence that the IMF in the Galactic Centre region is much flatter than that in the Galactic disk.

3. Formation and evolution of galactic nuclei and black holes

Text taken from Phase A study (not updated; technical specifications in Appendix are; ET edited text & changed a lot [reorganised] – I think it needs to be more quantitative and explicit in what are the interesting measurements to be made.) 20/9/16
Coordinator: Jens Thomas/MPE Maximilian Fabricius
Technical Templates: A.3, A.4 (Imaging); A.5 (Spectroscopy)

3.1 Background information

Among the long standing important issues in galaxy evolution are galactic nuclei and their supermassive black holes: how they form and evolve, and how their properties depend on and/or affect the galaxies around them. These issues range from the formation of galaxy cores, central star clusters and supermassive black holes, to the mechanisms of mass transport into these central regions and the influence of the galaxy-scale and larger environment. A suite of different mechanisms are expected to be at work, spanning nine orders of magnitude in linear scales from galaxy environment down to the sphere of influence of a central black hole. We still don't know if QSO/AGN feedback is the physical process that quenches star formation as massive star forming galaxies evolve into passive spheroids. Nor do we know which are the physical processes that can trigger nuclear activity. The role of environment (via interactions and/or merging) is still unsure. MICADO can address all these questions with its combination of diffraction limited resolution, high flux sensitivity and relatively wide field of view.

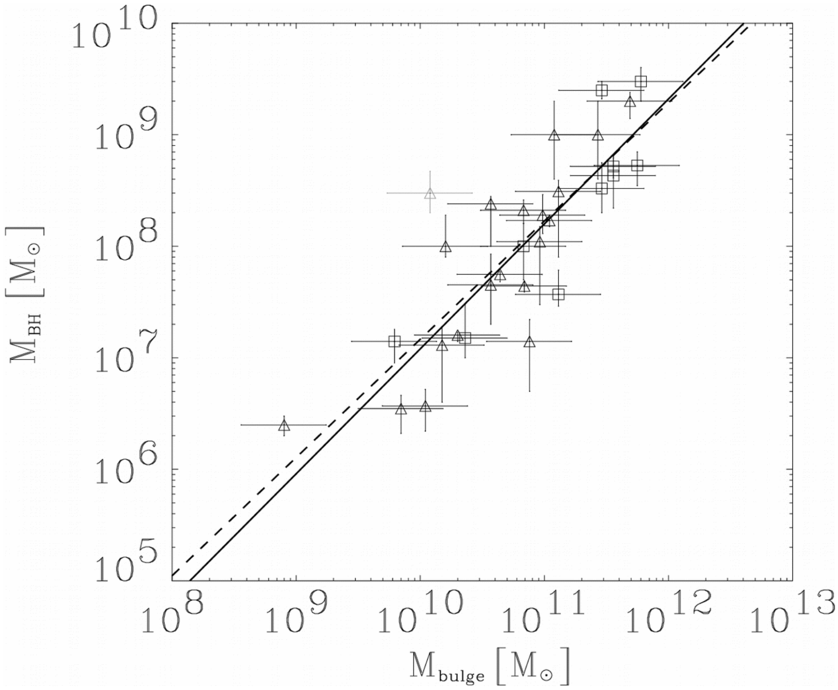

Figure 3.1: The empirical relation between the masses of nearby galactic bulges and their central black holes. An almost perfectly linear relation is found, with the black hole mass being 0.14±0.04% of the mass of the bulge (at bulge mass 10^{10} M_{sun}). Galaxies and their central black have to co-evolve. From Häring & Rix 2004, ApJ 640, L89. UPDATE?

The central structure and supermassive black holes in nearby galaxies: Mergers of Elliptical and early-type Spiral galaxies implies mergers of central black holes. While dynamical friction quickly leads to the formation of a compact black hole binary, the timescale over which this binary merges into a single black hole is highly uncertain. Hints for binary black holes have been found in a few cases at large distance only (e.g. OJ 287, Valtonen et al. 2008) but a systematic high resolution survey of nearby galaxy nuclei could produce highly interesting nearby candidates.

In the past decade, HST observations of local early-type galaxies have shown that two types of cores are present in these objects, correlated with absolute luminosity, kinematic anisotropy and isophote shapes of the galaxy. But we don't know why? While early-type galaxies brighter than MB ~ -21 have well resolved so-called cuspy cores, fainter ellipticals and bulges have power-law centres that, at the distance of Virgo and with the optical resolution of HST, appear unresolved (Lauer et al. 2007). Supermassive black holes have been detected in these galaxies, which are expected to have a (destructive) influence on their surroundings (Merritt et al. 2007).

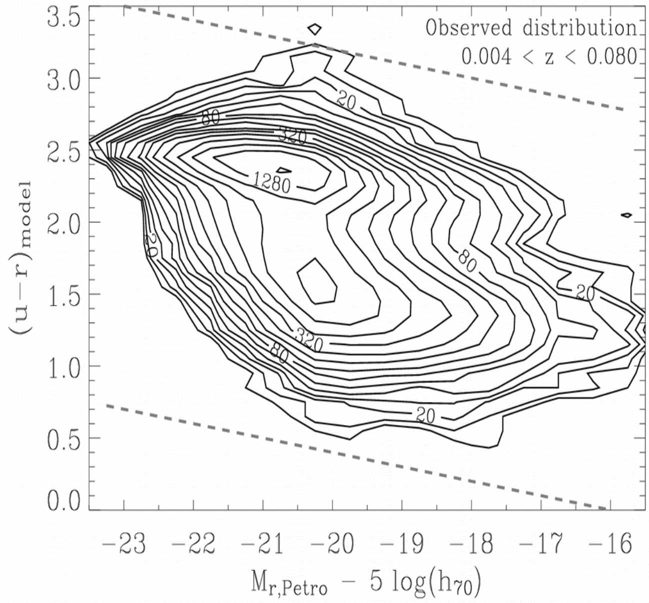

Figure 3.2: Bimodality in the colour–magnitude distribution of nearby galaxies (higher luminosity runs to the left, colours get bluer upwards). Shown are density contours from ~68000 galaxies in the redshift range 0.004<z<0.080 from the Sloan Digital Sky Survey. The ridge around colour (u-r)=2.5 is the "red sequence" of early type galaxies, the bluer distribution around (u-r)=1.5 is the "blue cloud" of star forming galaxies. In between lies the "green valley" where the space number density is lower. From Baldry et al. 2004, ApJ, 600, 681. UPDATE?

QSO Host Galaxies: More than a decade ago it was discovered that massive galaxies all appear to contain a supermassive central black hole, with a tight relation between the mass of the black hole and the stellar mass of the galaxy's bulge. With a ratio of ~1:1000 and with only 0.3 dex scatter, this relation suggests that the evolution of galaxies and their central black holes are linked (Figure 3.1). Moreover, this connection requires a mechanism that connects mass build-up in regions different by 10^9 in linear scale. And so?

Another major unresolved issue in present day extragalactic astrophysics is that the apparent transformation from a massive star forming galaxy "blue cloud" to "red sequence" galaxies that no longer are able to form stars. The colour–magnitude or stellar-age–mass diagrams of galaxies that show these two major populations is shown in Figure 3.2. In the "blue cloud" a major fraction of the total stellar mass in the universe is created. Most of these galaxies are disks with substantial gas reservoirs. On the other hand, a substantial fraction of this stellar mass will eventually end up in galaxies on the "red sequence" of early type galaxies. Galaxies here are dynamically hot, have little available cold gas, and hence have a low level of or no star-formation at all. Both populations are prominent, with a dip between them. Puzzling is the sparseness of transition objects: If the gas reservoirs of star-forming disk galaxies are used up by continuous depletion via star formation, then the time a galaxy takes to transverse from the blue cloud to the red sequence would be several Gyr, too long for the two disjoint populations to actually be discernable.

Thus, the existence of the bimodality in Figure 3.2, requires a much more rapid truncation of the star-formation for a disk galaxy and subsequent transition to the red sequence on a timescale of order of 1 Gyr. One plausible mechanism to truncate star-formation could be energetic feedback from the supermassive black hole into the galaxy, or AGN feedback. The strong accretion or "quasar" phase dominates the mass growth of galactic black holes. The total amount of energy emitted by an active galactic nucleus during such a phase is higher than the gravitational binding energy of matter in its surrounding galaxy. This can a) stop star-formation by heating the gas sufficiently or by physically driving it out of the galaxy, and b) regulate the mass growth in the galaxy in connection with black hole properties.

What is needed is a precise empirical determination of the actual bulge mass to black hole mass relation and its evolution since the early Universe. This would constrain possible physical mechanisms connecting bulge and black hole. The few currently existing studies sample very few targets and do not span a substantial mass baseline. Only two studies reach a redshift of beyond 2. Still true? Perhaps add something more aimed specifically at MICADO…

QSO Environments: Quasar environments have been studied on different scales ranging from those of the host galaxy to cluster? scales. Such studies have provided important but controversial results regarding the environment of quasars. It has been known for more than three decades that quasars are associated with enhancements in the spatial distribution of galaxies. These studies have shown that in the nearby universe, quasars reside in environments ranging from small to moderate groups of galaxies rather than in rich clusters (Bahcall & Chokshi 1991b; Fisher et al. 1996; McLure & Dunlop 2001). These findings suggest that quasars are located in over-dense regions, more so than L* galaxies, since higher over-density regions are clustered more strongly than lower (e.g. Kaiser 1984; Bardeen et al. 1986). An over-dense environment would indeed be expected if the quasar activity were triggered by galaxy interactions. To develop a better understanding of the quasar phenomenon, it is therefore important to investigate and quantify the relation amongst nuclear activity, host galaxies and the associated environments.

All systematic studies of the properties of QSO environments refer to low redshift ($z < 0.5$) objects. The most extensive studies were carried out by Serber et al. (2006) and Strand et al (2007), based on the SDSS archive. From a large dataset of $z < 0.4$-0.6 quasars, they found that luminous objects are located in higher local over-density regions than typical L* galaxies.

Only for a few selected fields around high-z quasars has the environment been explored (Bornancini et al 2007; Coil et al 2007; Stockton et al 2006). This limitation hinders the possibility to investigate the cosmic evolution of environment and thus to have a full understanding of its role in driving nuclear activity. It is thus of crucially important to study the environments of QSOs at epochs corresponding to the peak of QSO activity and beyond. With the current 8-10m class telescopes this is not possible because inadequate sensitivity and spatial resolution.

3.2 Importance of MICADO

[this is copied and adapted – slightly- from 3.1] MICADO & EELT are well suited to the study at optical/IR wavelengths of the black holes at the centres of most (all?) galaxies. This is zone where the highest spatial resolution is required, and exquisite photometry to be able to distinguish the properties of any accretion disc and the surrounding star formation properties and how they are affected by the presence of a black hole at various stages of activity. In some cases it might also be possible to see the stars move, in external galaxies, as is already seen in the Galactic centre. This will probably be matched to HARMONI? At that level of precision a number of key issues of the physics of massive black holes and their surroundings can be tackled. MICADO research on black holes in nearby galaxies will likely concentrate on the following issues:

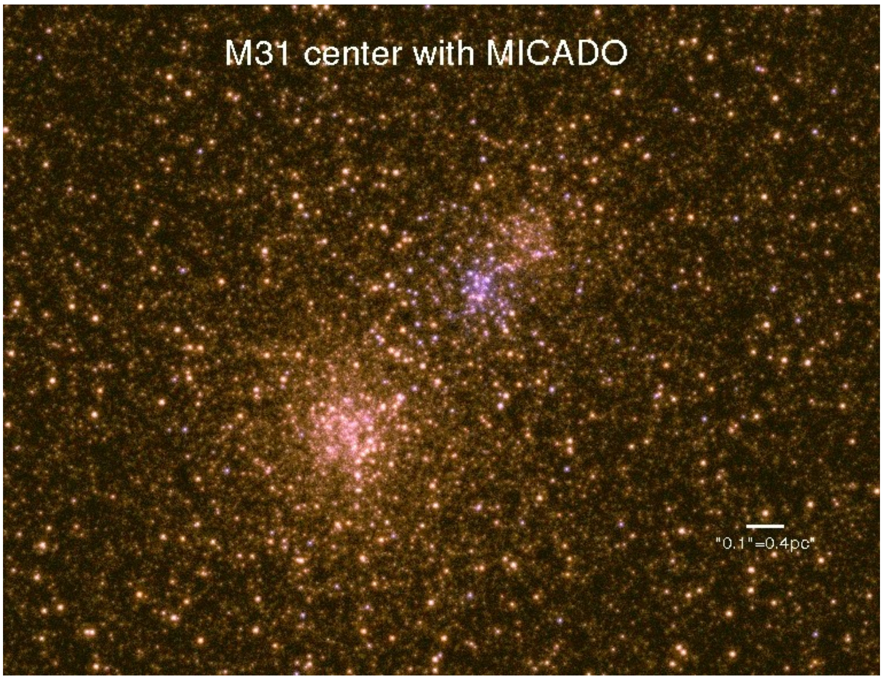

Figure 3.3: The core of M31 at the resolution of MICADO, using an HST PSF scaled to the MICADO resolution. The image has 3 mas size pixels and is ~2.5 arcsec on the side. Keep? or redo? It is very pretty.

- MICADO imaging is needed to resolve the power-law cores and measure their core radii of black holes in the centres of nearby galaxies How nearby/what masses - details. MICADO at the ELT will be able to achieve 0.01 arcsec wide field – is narrow useful? resolution in the K band with optimal AO and thus detect core radii down to approximately one pc at the distance of Virgo. Is there a prediction that this is enough?

- MICADO will allow the detection of rings and disks in the nuclei of galaxies closer than Virgo, similar to the ones seen in the Milky Way and M31 (Bender et al. 2005; 2009) and also extremely compact bar-type structures like the one found in NGC 3706. Which will tell us? For example, the (blue) nuclear disk detected in M31 would be resolvable out to a distance of 7 Mpc (see Figure 3.3). HOW does Figure 3.3 show this? The presence of eccentric nuclei will be detected at twice this distance or even in Virgo. Why? Additional J or H band imaging will measure the associated colour gradients to constrain the stellar populations of the nuclear region.

- At smaller distances HOW SMALL, it should be possible to resolve single red super-giants in circum-nuclear disks. For example if Cen A, at a distance of 4.3 Mpc, has a central disk of blue stars similar to M31, it will be possible to resolve 5-10 super-giants in that disc (plus a background population of a few dozens old supergiants along the line-of-sight). Is this convincing? Is this not a HARMONI case? The disc would have an area ~ 0.05 arcsec^2 at this distance. Both old and young how old? How young? stars are bright enough (J=-3 to -5, J-H=1 for the former, 0.5 for the latter type) that their colours can be measured and used to distinguish the two populations. Why useful? Assuming that the astrometric position of these red supergiants can be measured with a precision better than 1/3 of a pixel mas (for 3 mas pixels), or 0.02 pc in Cen A, one can detect the motion of a star moving at 2000 km/s over a period of 10 years. High resolution vs. standard resolution imaging? Probably all will done in HR mode, or SCAO??

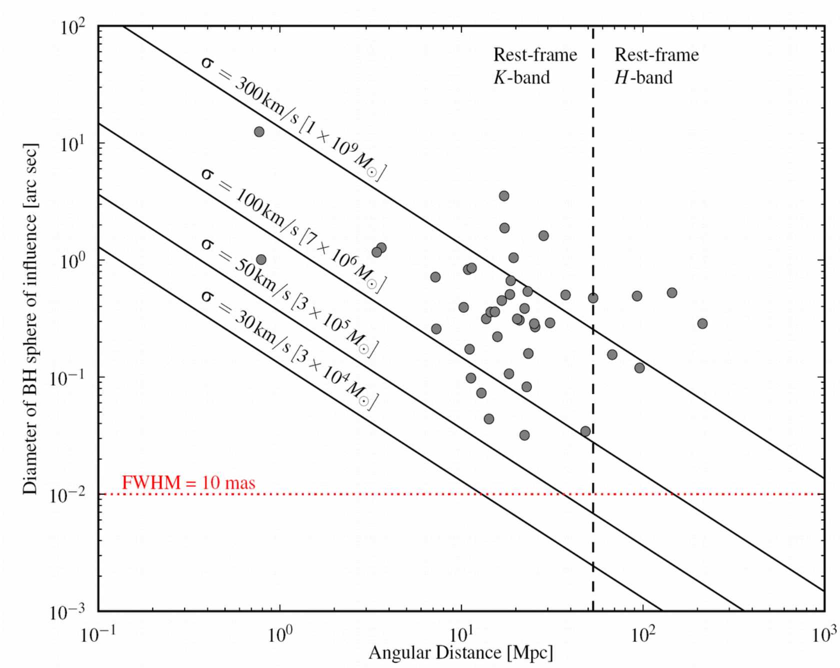

Figure 3.4: The size of the sphere of influence of a black hole as a function of its mass and distance. The red dotted line shows the spatial resolution achievable with MICADO. If you only need a field of 20 arcsec – then MICADO can do better in zoom mode.

- The resolution and light collecting power of an ELT will also allow the detection of flares in nearby galaxy nuclei that are similar to the ones observed in the Milky Way (Trippe et al. 2007).

- The availability of spectroscopy what kind? together with the astrometric data allows the complete reconstruction of the orbits, similar to what has been done for the Galactic centre. The radial velocities of resolved stars could allow the mass determination of intermediate mass black holes. In addition, the stellar kinematics of the (unresolved) centres of galaxies could be measured. A spectral resolution of R~5000 makes it is possible to measure velocity dispersions (σ) as low as 20 km/s. Figure 3.4 shows the sphere of influence of a black hole of a given mass as a function of angular distance, and we show galaxies with black hole mass determinations from stellar and gas kinematics. At the moment direct measurements are lacking at the low σ end, and are essentially limited to the nearest galaxies. MICADO will be able to spatially resolve the dynamical influence of "seed black holes" in local inactive bulge-less or dwarf galaxies out to ~50 Mpc and the supermassive ones of inactive massive Ellipticals out to redshift z~0.35.

- The projected space density of galaxies hosting quasars is low. Combining all redshifts, there are few per square degree, and even fewer for particular target redshifts. Thus, MICADO with a field-of-view of >100 kpc at z=2, corresponding to >15 arcsec is a perfect match to observe quasar galaxies individually. Resolving and measuring properties of the host galaxy around a bright nucleus is not limited by observable depth, but by how well the nuclear light can be characterized in an image. The limits are thus given by a combination of contrast between nucleus and host galaxy brightness, PSF width and the precision to which the PSF shape can be characterized. I guess with its extremely high spatial resolution MICADO will be very good at this?

- An example of a simulated host galaxy that contains a 5 times brighter (brighter than what? The galaxy?) active nucleus observed in the H-band, assuming an external seeing of 0.8", is shown in Figure 3.5. The galaxy is spheroidal with r_0 = 3kpc at redshift z=3. This corresponds to r_0 = 0.38 arcsec. The radial surface brightness profiles of the models are shown in Figure 3.6. The technical objective is to measure the difference between the nuclear emission and the total emission. In the absence of noise this requires a precision that corresponds to the ratio of nuclear and galaxy emission. This precision varies as a function of radius, as it is directly related to the relative strength of the nucleus compared to the galaxy. A doubling of this ratio will reduce the uncertainty by a factor of 2. The precision is also affected by how well the PSF is known, that is how well the flux of the nuclear component can be determined. If the radial shape of the PSF envelope is similar to that of the host galaxy, then it is only the core that can be used to infer the relative nuclear point source contribution. In this case the precision will be dominated by the exact knowledge of the Strehl ratio at the location of the QSO at the time of observation. This means knowledge of the PSF shape to a few per cent.

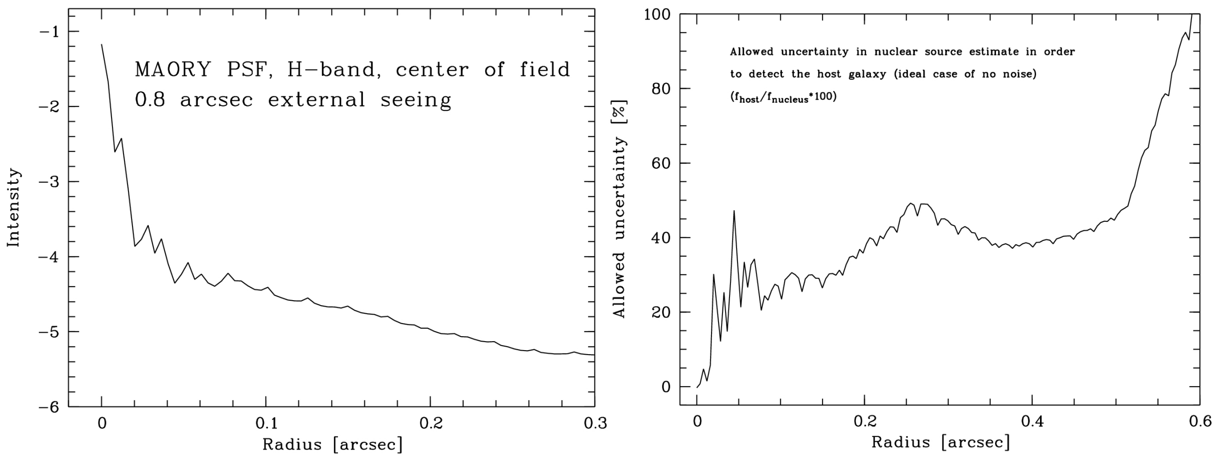

Figure 3.5: Left panel: radial surface brightness profile of the MAORY PSF. Right panel: allowed uncertainty of the nuclear point source at each point in the noise-free case. This uncertainty is the product of uncertainty in PSF shape and the ability to determine a scale factor.

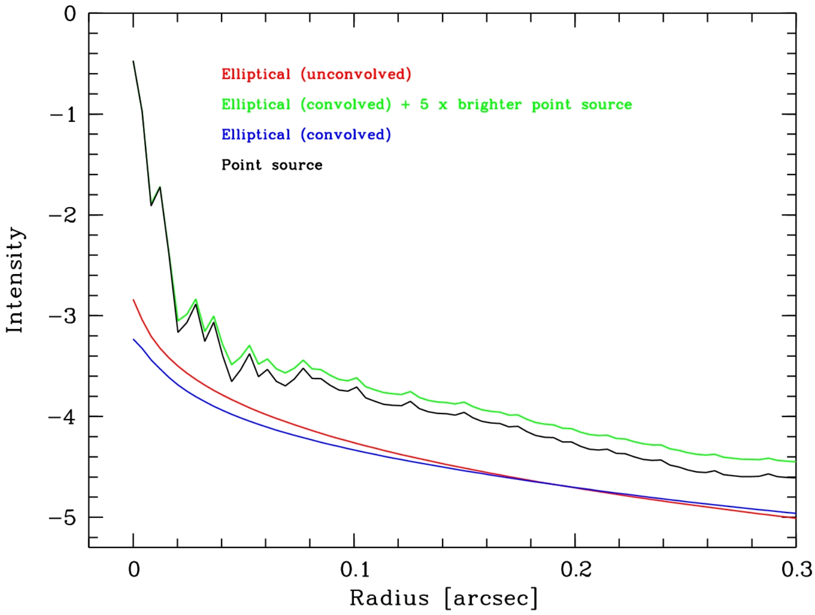

Figure 3.6: Simulated elliptical galaxy before (red) and after (blue) convolution with the PSF. If a 5 times brighter point source (black) is added, the total profile (green) is produced.

This is obviously not my field – but this plot makes me wonder way you care about the galaxy? Is this a good test case?

- To study QSO environments at z=2-3 need to observe galaxies of M > M* and thus it is necessary to detect objects with K > 24-25. Assuming a cosmic evolution of the physical radius, these galaxies will have an angular size of 0.2-0.4 arcsec . Under these conditions it is possible to detect these faint (K ~ 25) galaxies with integration times of a few hours. The excellent spatial resolution of E-ELT+MICADO will also allow one to detect any signature of interactions for the galaxies closest to the QSO, and thus obtain fundamental data to assess the role of interaction and mergers in the activation and fueling of the QSO phenomenon at the epoch of its maximum.

4. Galaxy Evolution

Coordinators: Natascha M. Förster Schreiber /MPE & Simona Mei /Obs. Paris (this version: 27/10/2016).
Contributors: Piercarlo Bonifacio, Renato Falomo, Leon Koopmans, Mathieu Puech (with M. Gullieuszik, L. Greggio M. Huertas-Company) correct? Leon will send some lensing.
Technical Templates: A4.6, A4.7, A4.8 (Imaging); A4.9 (spectroscopy)

The field of galaxy evolution has undergone major developments in the past two decades, with the confluence of unique instrumentation and techniques that have opened up the z > 1 Universe to observational studies, and with computational power that has enabled ever more sophisticated numerical simulations. We now have a fairly robust outline of the evolution of the global galaxy properties over much of the Universe's history, and first tantalizing pieces of evidence of *how* galaxies assembled and transformed into the present-day Hubble sequence. The next obvious step is to resolve these faint distant galaxies on sufficiently small physical scales to characterize accurately their sub-galactic components. This Section outlines key outstanding questions that can only be answered with sensitive observations at very high spatial resolution as will be afforded by MICADO, the first-light diffraction-limited imager and spectrograph at the E-ELT.

4.1 Background information

The mechanisms driving galaxy formation and evolution involve a complex interplay between hierarchical merging of dark matter halos, the accretion and cooling of gas, gravitational fragmentation and the formation of molecular clouds, the resulting star formation, nucleosynthesis, and metal-enriched outflows (feedback) that are driven by stellar winds, supernova explosions and energetic output from accretion onto supermassive black holes (AGN activity). Recent developments have shown that $\gtrsim\gtrsim$ 90% of star-forming galaxies (SFGs) out to lookback times of 11 billion years (redshift z~3) exhibit a tight relation between their star formation rate and their assembled stellar mass (e.g., Daddi et al. 2007; Whitaker et al. 2014) and consist of a majority of disks that are increasingly star-forming, gas-rich, clumpy, and turbulent as a function of look back time (e.g., Wuyts et al. 2011; Tacconi et al. 2013; Wisnioski et al. 2015). In the "equilibrium growth" picture suggested by these results (e.g., Lilly et al. 2013), the elevated star formation rates of early galaxies are sustained by a fairly continuous supply of fresh gas from the cosmic web that maintains large gas reservoirs. This cosmological gas inflow is balanced by the rate at which stars form from cooled gas and gas is blown out of galaxies. The early turbulent gas-rich disks are marginally stable, fragmenting into giant gas/star-forming complexes with a size that scales with gas content. Once galaxies grow above 10^{11} $M_\odot$, their star formation is quenched, possibly due to one or more of: a sudden drop in the gas cooling in haloes, a drop in star formation efficiency within galaxies, the removal of gas via galactic winds, or the stabilizing action of growing bulges. While the statistical census of deep surveys, that look back to the distant past, plays an important role in establishing the broad scope of scenarios such as the "equilibrium growth model", more detailed spatially- and spectrally-resolved studies of individual galaxies are critical to improve our understanding of the physical processes at play. It is clear that as accurate as our studies are today, they are not able to trace the small spatial scales required to comprehensively follow the structural and stellar mass growth of galaxies.

Current studies of resolved galaxy morphologies and colours out z ~ 3 reached their peak with the advent of the WFC3 camera on-board the Hubble Space Telescope (HST), which extended our detailed view of evolving galaxies from the optical to the near-IR window probing the rest-frame optical emission from the bulk of stars at this redshift. In parallel, integral field spectrometers such as SINFONI, KMOS, and MUSE at the VLT routinely map the ionized gas kinematics and physical conditions of galaxies out to z ~ 3, see Figure 4.1. With HST and ground-based AO-assisted observations, one can achieve an angular resolution of 0.1″–0.15″, corresponding to a physical scale of ~ 1 kpc at z > 1. The deepest observations enable us to probe galaxies during the first two billion years after the Big Bang, with the detection of many hundreds of candidate galaxies well into the epochs of reionization (z > 7), and even the spectroscopic confirmation of a handful at z > 8 (e.g. Oesch et al. 2015). At submillimeter to radio wavelengths, ALMA, NOEMA, and E-VLA have just begun to bring resolved studies of the cold gas and dust reservoirs of galaxies on par with those of their stellar and ionized gas components.

Due to our limits in spatial resolution the current picture remains incomplete because: (i) the best resolved physical scales are ~ 1 kpc at z > 1 (with the rare exceptions of strongly-lensed objects); (ii) the low-mass ($\log(M_*/M_\odot) < 10$), but abundant, galaxy population is largely missing and (iii) the detailed properties for galaxies at $z > 3$, when galaxies were building up their first stars and gas reservoirs, are poorly explored. The next steps require a more detailed physical characterization of galaxies over a wider range of mass, star formation activity, and environment. This requires the giant leap uniquely afforded by the E-ELT, with its 39-m aperture and a 2μm diffraction limit of 13 mas (which is $\approx$100 pc at $z > 1$). It is important to stress that JWST's diffraction limit at 2μm is only 80 mas (which is $\approx$650 pc at z > 1). Moreover, the best spectral resolution offered by JWST spectrographs in the optical/near-IR will be modest ($R \lesssim 2700$, i.e., a velocity dispersion of $\sigma \gtrsim 50$ km/s). By exploiting the angular resolution and sensitivity of the E-ELT, *MICADO will take resolved studies of distant galaxies to the next level*, opening unprecedented opportunities to address outstanding questions in galaxy evolution.

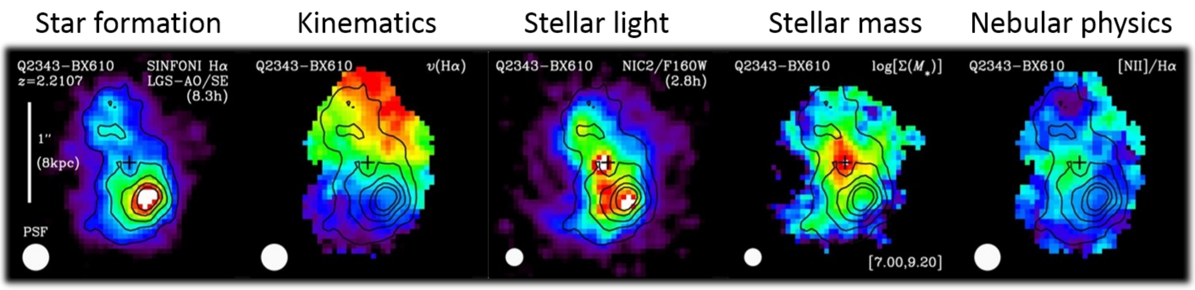

Figure 4.1: Different views of a massive SFG at z = 2.21, Q2343-BX610, revealed by SINFONI+AO observations in the K band and HST J and H band imaging (the cross marks the kinematic centre). With a PSF FWHM ≈ 0.2″, the data resolve detailed structures on ~ 1.5 kpc scales, notably bright off-centre star-forming clumps in Hα (left panel) and rest-optical continuum light (middle panel). The kinematics traced by the Hα line emission (second panel from left shows the velocity field) reveals that this object is a regularly rotating disk galaxy. The distribution of stellar mass inferred from the J-H colour map (fourth panel from left) further reveals the presence of a massive stellar bulge. Spatial variations in nebular line ratios (right panel shows the [NII]/Hα map) and in the emission line profiles imply enhanced excitation around the centre due to the presence of an outflow driven by a (low-luminosity) AGN, and a negative but shallow gas-phase oxygen abundance gradient towards the outer disk parts. Based on data presented by Genzel et al. (2014) and Tacchella et al. (2015).

4.2 Importance of MICADO

It is now fairly well established that a correlation between global galaxy structure and stellar population properties, the Hubble sequence, was already in place at z~2.5 among massive galaxies (e.g., Wuyts et al. 2011). It is however not understood how this came about and so rapidly, and what happens during the subsequent 11 billion years of cosmic time until the present day. Do galaxies form (and quench) inside-out? What is the rate of size growth of disks and spheroids? What is the role of mergers, internal dynamical processes, and feedback in galaxy growth? When and how do the thick disks, bulges, and globular clusters of today's galaxies form? How were the densest galaxies in the local Universe and out to z ~ 3 assembled? What did the progenitors of Milky Way-like galaxies look like in their first few billion years?

MICADO will enable deep views of galaxies across cosmic times that are 5–10 times sharper than possible currently and even with JWST. The smallest and faintest galaxies, as well as substructure within galaxies, will become accessible for study on scales of ~ 100 pc. Key science drivers for MICADO encompass a broad range of themes addressing fundamental aspects of the lifecycle of galaxies from the earliest times, and also the connection with the circum-/intergalactic medium and the dark matter.

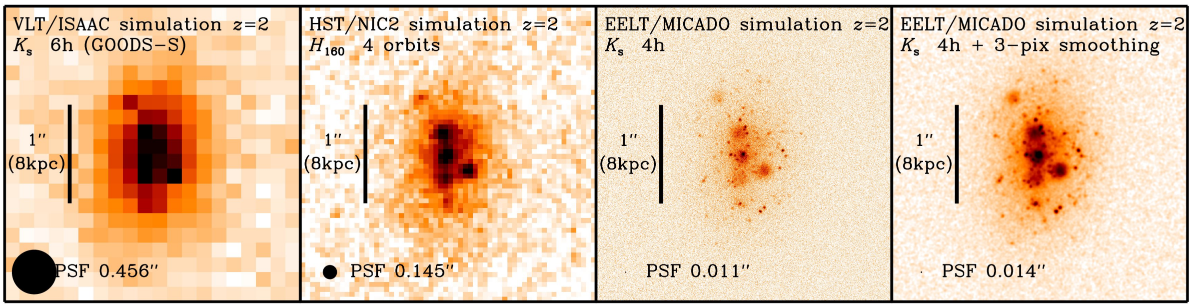

Figure 4.2: Illustration of the gain in resolution with MICADO at E-ELT. From left to right, the panels show a simulated z=2 galaxy in deep but seeing-limited ground-based observations (6 hours with VLT/ISAAC in K, equivalent to data of the GOODS-South field), deep diffraction-limited HST/NICMOS observations (4 orbits with NIC2 camera in H), and similar integration time of 4 hours with E-ELT/MICADO in K, at a resolution of about 10 mas or 80 pc at z=2 (10 times better than with HST, and 5 times better than with JWST). The mock galaxy was created so as to resemble a real bright and large galaxy (K_{AB} ~ 21.3 mag, half-light radius ~ 5 kpc) with very prominent clumpy structure (Q2343-BX610; see Figure 4.1; Förster Schreiber et al. 2011; Genzel et al. 2014), including a smooth underlying component and several kpc-sized clumps. In addition, a few hundred compact (unresolved) clusters were added with a range of magnitudes. The clumps and clusters contribute roughly 40% of the total light of this simulated galaxy. Compact clusters to K_{AB} ~ 28.5 mag are well detected; this brightness corresponds to an absolute magnitude in the rest-optical of R_{AB} ~ –16 mag, and is comparable to the most luminous "super star clusters" in nearby starburst galaxies such as M82 and the Antennae. Small amount of smoothing (with a Gaussian of FWHM equal to that of the PSF) enhances the rich structure one might be able to detect with such MICADO observations.

Resolving disks at high redshift: The detailed workings of the physical processes at the origin of the early Hubble sequence remain elusive. The main limitation is spatial resolution (see Figure 4.2). Current observations of faint high-redshift galaxies achieve at best 0.1″–0.15″ FWHM resolution (~1 kpc at $z > 1$). This resolution roughly corresponds to the typical radii of $\log(M_*/M_\odot)$ ~ 9 star-forming galaxies and $\log(M_*/M_\odot)$ ~ 10.5 quiescent galaxies, and to the inferred vertical height of star-forming disks at z ~ 2. High resolution imaging with HST generally gives very few resolution elements, of order 10 within an effective radius. This is equivalent to imaging Virgo galaxies with 10″ seeing. Morphological features such as star-forming clumps and putative bulges can be viewed on only ~1 kpc scales and so the detailed profiles cannot be determined.

One of the most striking feature in the morphologies of z > 1 galaxies is the frequent presence of giant kpc-scale, luminous ``clumps'', see Figures 4.1 and 4.2. The discovery of these large clumps in the first deep extragalactic optical imaging surveys with HST lent support to the idea that galaxy formation and evolution are dominated by early mergers (e.g. Cowie et al. 1995). High-redshift galaxy disks also differ from present-day disks in that they have 10–20 times higher global star formation rates, are several times more gas rich, and are characterized by a more turbulent ISM with up to ~10 times higher intrinsic disk velocity dispersions, σ_0. The ratios of rotation velocity, v_{rot}, to dispersion are typically of order ~1–10, implying that high-z disks are also geometrically thicker than local spirals, which have v_{rot}/σ_0~10–20. These results raise many questions about the nature and timescales of internal dynamical processes at the epochs when thick disks, bulges, and metal-rich globular clusters were forming. To address these questions, in the necessary detail, images are needed with the high resolution that only MICADO can provide.

With its much larger collecting area and smaller pixels scales, the E-ELT with MICADO will achieve a factor ~10 improvement in spatial resolution compared to HST and JWST instrumentation hence providing multi-colour images of high-redshift galaxies with a richness of detail approaching what is currently only possible for relatively nearby galaxies. This leap in resolution and sensitivity will make it possible to map the distribution of stellar light on scales of ~100 pc or better. This will make it possible to distinguish bulge and disk components and measure their sizes and detailed structural profiles. It will also allow the search for luminous star clusters, for signatures of AGN activity. This will make it possible to pinpoint the physical processes that are shaping galaxies at the epoch when mass build up and morphological differentiation are at their peak. Diffraction-limited imaging with MICADO will typically provide >100 resolution elements across galaxies, and this will make it possible to isolate and even resolve regions with sizes comparable to individual star-forming complexes such as 30 Dor in the LMC and N66 in the SMC. In addition slit spectroscopy with MICADO on these spatial scales, with R ~ 10k spectral resolution, will allow measurements of the kinematics of clumps down to 100pc size, providing their dynamical masses. For example a 10^8 $M_\odot$ clump of 500 pc radius would have an emission line width of σ ~ 15 km/s. High-resolution slit spectroscopy will further help to determine if there is evidence for rotational-support as some simulations suggest (e.g., Ceverino et al. 2012). The rest-frame optical emission line spectra of clumps will enable measurements of their metallicities and gas mass outflow rates driven by star formation, further constraining their origin (in-situ vs. external) and their long-term fate.

Looking for signs of bulge formation: The presence of genuine "bulges" in massive high redshift disks remains uncertain. The central excess in stellar light/mass detected in HST imaging, most pronounced for higher mass galaxies, is barely or not resolved in current observations, such that it is unclear whether the associated structure is a classical bulge (with a $R^{1/4}$ de Vaucouleurs profile), or a pseudo-bulge or inner disk (and a shallower profile). The detailed profiles of galactic components carry the imprint of the formation mechanism (e.g., Kormendy 2016; Bland-Hawthorn & Gerhard 2016). MICADO high-resolution imaging will for the first time resolve the inner regions (R < 1 kpc) of massive galaxies and shed crucial light on the mechanism(s) and timescale for the formation of bulges. High-resolution spectroscopy will constrain the dynamical state (dominant rotation vs pressure support) and total enclosed mass as a function of radius on unprecedented scales in and around the nuclear regions. Spectroscopy would further pin down the origin — AGN or compact nuclear starburst — of the powerful "nuclear outflows" (through FWHM ~ 500 – 2000 km/s broad wings in nebular emission lines) recently discovered in a majority of galaxies at/above the Schechter mass, which are thought to play a role in quenching of high-mass galaxies.

Looking for Globular cluster formation: Metal-rich globular clusters in nearby galaxies are known to be dynamically associated with their bulges and thick disks. The ages and abundance patterns of these globular clusters suggest an early formation a few billion years after the Big Bang (e.g., Searle & Zinn 1978). These properties, together with the typical distribution and kinematics of globular cluster populations, have led to the suggestion that the giant clumps seen in z ~ 2 star forming galaxies may be emerging globular cluster populations (e.g., Shapiro et al. 2010). MICADO will directly test this scenario, by resolving the structure of clumps and determining their kinematics. This experiment has demanding requirements for MICADO, in terms of image stability, resolution and sensitivity, see Figure 4.2. To be able to characterize clump substructure above the host galaxy luminosity requires a very well determined PSF with the highest possible strehl. MICADO imaging simulations with a PSF FWHM of 100 pc and Strehl of 50% suggest that compact putative GC progenitors could be detected (S/N ~ 3) up to K_{AB} = 28.5 mag, see Figure 4.2. At z ~ 2, this sensitivity corresponds to a rest-frame absolute R-band M_{AB} = –16 mag, which is about that of the most luminous "super star clusters" in local starburst galaxies such as M82 and the Antennae. Sensitive high spatial and spectral resolution spectroscopy with MICADO, would allow an estimate of the dynamical masses of such young luminous stellar clusters. For example, a 10^7 $M_\odot$ cluster with a 50 pc radius would have an emission line width, σ ~ 15 km/s. Their chemical abundances can be measured from strong emission lines.

Resolving compact galaxies at z>2: Recent results have shown a population of compact galaxies at z>2 (Daddi et al. 2005; Cimatti et al. 2008; van Dokkum et al. 2008; Huertas-Company et al. 2013, 2015; van der Wel et al. 2014, and references therein), consistent with part of the galaxies increasing their size by minor mergers (Naab et al. 2009; van Dokkum et al. 2010; Shankar et al. 2013, 2014) and part quenching at later time (Carollo et al. 2013; Stringer et al. 2013). We still do not understand how these galaxies formed. They are four times more compact at z~4 than compact galaxies in the local Universe, and they show both quiescent and star-forming stellar populations (Barro et al. 2013, 2016; Mei et al. 2015). The star-forming compact galaxies number density drops at z>3 (with only 15% of compact galaxies being passive at these redshifts; Marchesini et al. 2014; Williams et al. 2014), indicating that they are quenched between z~2 and z~3. These galaxies will be marginally resolved with the JWST. On the contrary, MICADO will resolve them, identify signatures of mergers, and obtain precise radial profiles to understand where and how quenching happens.

Progenitors of massive ETGs in the densest environments: The galaxies found in clusters are very different from the field up to z~1.5 (e.g. Mei et al. 2009). In galaxy clusters, ~80% of the galaxies have early-type morphology (elliptical and lenticular galaxies with large bulges and minor or no disks) with on average old stellar populations. This is in contrast to the field, where ~80% of the galaxies have late-type morphology (spiral galaxies with small bulges and large disks, and irregular galaxies) and are still forming stars. These fractions dramatically change at z>1.5, where star-forming galaxies significantly populate cluster cores (Brodwin et al. 2013; Mei et al. 2015; Alberts et al. 2016; Noirot et al.2016), indicating both stellar population and morphological transformations at this epoch. The high resolution imaging from MICADO will permit us to study in detail the structure of the galaxies found in young clusters and proto-clusters at z>1.5 and discriminate physical mechanisms behind their transformations (e.g. mergers, disk instabilities). These cannot be resolved with current HST imaging in which they appear as blurred irregular features (see Figure 4.3). To study detailed morphology and identify mergers, we require a resolution of at least 10mas to distinguish low mass merger partners and low surface brightness features. This is beyond HST and JWST capabilities. A magnitude depth of ~28 AB is necessary to identify galaxies brighter than L* at the higher redshifts. Thus, only MICADO will be able to detect such low surface brightness features, identify potential mergers, and disturbed morphologies at the needed scale of ~100pc. Spectroscopy will be able to separate multiple companions and confirm the structures to originate from mergers.

Structure of strongly lensed galaxies and dark matter halo substructure: Strong gravitational lensing provides a potentially powerful channel through which mass (sub)structure in galaxies can be detected and quantified in an unbiased way over a wide range of masses and redshifts. Surface brightness anomalies provide the most reliable method to assess the level of (dark matter) substructure in galaxies, however this approach relies on deep, high spatial resolution observations (e.g., Vegetti et al. 2014). MICADO will lower the currently attainable mass limit by an order of magnitude down to $\sim 10^7 M_\odot$, well within the regime of nearly dark satellites as currently seen around the Milky Way, for galaxies out to redshifts z>1. At these masses, each lens galaxy is expected to exhibit one or more surface-brightness anomalies given current CDM predictions. This science case also has broad synergy with EUCLID, as this European "lens factory" is expected to discover $>10^5$ new lenses, and the follow-up of a selected sub-sample of these lenses with MICADO will enable an accurate probe of the evolution of dark matter substructure over a wide range of galaxy masses, types and environments.

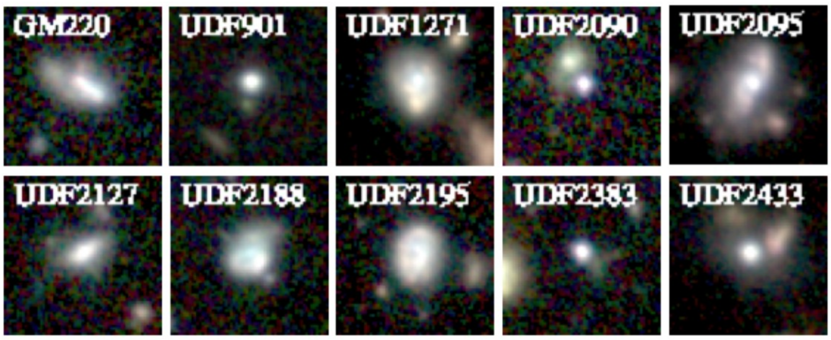

Figure 4.3. Example of galaxies in clusters at z~2, from Mei et al. (2015): combined colour images of the spectroscopically determined members of the proto-cluster HUDFJ0332.4-2746.6 at z~1.84, from HST/ACS and WFC3 images. Most show asymmetries, faint substructures and tails, which are most likely signatures of mergers.

References:

Alberts, S. et al. 2016, ApJ, 825, 72; Barro, G. et al. 2013, ApJ, 765, 104; Barro, G. et al. 2016, arXiv:1509.00469; Bland-Hawthorn, J. & Gerhard, O. 2016, ARA&A, 54, 529; Brodwin, M. et al. 2013, ApJ, 779, 138; Carollo, M. et al. 2013, ApJ, 773, 112; Ceverino, D., et al. 2012, MNRAS, 420, 3490; Cimatti, A. et al. 2008, A&A, 482, 21; Cowie, L. L., Hu, E. M., & Songaila, A., 1995, Nature, 377, 603; Daddi, E. et al. 2005, ApJ, 631, L13; Daddi, E., et al. 2007, ApJ, 670, 156; Förster Schreiber, N.M., et al. 2011, ApJ, 739, 45; Genzel, R., et al. 2014, ApJ, 785, 75; Huertas-Company, M., Mei, S. et al. 2013, MNRAS, 428, 1715; Huertas-Company, M., Pérez-González, P. G., Mei, S. et al. 2015, ApJ, 809, 95; Kormendy, J. 2016, Astrophysics & Space Science Library, 428, 431; Lilly, S. J. 2013, ApJ, 772, 119; Marchesini, D. et al. 2014, ApJ, 794, 65; Mei, S., et al. 2009, ApJ, 690, 42; Mei, S., et al. 2015, ApJ, 804, 117; Naab, T. et al. 2009, ApJL, 699, 178; Noirot, G. et al. 2016, ApJ, in press; Oesch, P. A., et al. 2015, ApJ, 804, L30; Searle, L. & Zinn, R. 1978, ApJ, 225, 357; Shankar, F. et al. 2013, MNRAS, 428, 109; Shankar, F., Mei, S. et al. 2014, MNRAS, 439, 3189; Shapiro, K. L., Genzel, R., & Förster Schreiber, N.M. 2010, MNRAS, 403, L36; Stringer, M.J. et al., 2014, MNRAS, 441, 1570; Tacchella, S., et al. 2015, ApJ, 802, 101; Tacconi, L. J., et al. 2013, ApJ, 768, 74; van der Wel, A. et al. 2012, ApJS, 203, 24; van Dokkum, P. G. et al. 2008, ApJL, 677, 5; van Dokkum, P. G. et al. 2010, ApJ, 709, 1018; Vegetti, S., et al. 2014, MNRAS, 442, 2017; Whitaker, K. E., et al. 795, 104; Williams, C. et al. 2014, ApJ, 780, 1; Wisnioski, E., et al. 2015, ApJ, 799, 209; Wuyts, S., et al. 2011, ApJ, 742, 96

5. Astrometry of Globular Clusters and Dwarf Spheroidal Galaxies

Text rewritten (ET), but making use of Phase A study & text from Davide; edited Koen & Davide (Oct 2016).

Coordinator: Koen Kuijken/Eline Tolstoy (NOVA) .
Contributors: Massari, Tolstoy, Helmi, van de Ven; Pott; Nicklas,Dreizler, Kamann *Technical Templates: A.10, A.11 (Imaging)*

5.1 Outstanding Questions

Nearby galaxies and globular clusters are important probes of dark matter and its distribution in the Milky Way and the Local Group [e.g. Mateo 1998; Battaglia et al. 2005]. These stellar systems have a variety of different masses and distances [Harris 1996; McConnachie 2012]. Proper motion measurements will allow us to determine both the internal velocities and the orbital motions of the satellites of the Milky Way and potentially beyond. The nearby dwarf galaxies are the smallest systems where dark and visible (baryonic) matter co-exist, and thus they represent the benchmark to study how the presence of dark matter affects the evolution of visible matter [e.g. Tolstoy et al. 2004; Battaglia et al. 2008; Walker et al. 2009], and even possibly to set constraints on the physical nature of dark matter particles. These works clearly show the critical need for proper motion studies to break the degeneracy in the interpretation of the radial velocity measurements. Dwarf galaxies are typically further away than globular clusters, which are often in reach of HST astrometric studies [e.g. Massari et al. 2013; Bellini et al. 2014] see Figure 5.1. Dwarf galaxies as more distant satellites are also fundamental as dynamical probes of the extended gravitational potential in which they move, to accurately determine the total mass and shape of the Milky Way [e.g. Vera-Ciro & Helmi 2013] and the Local Group. ESA/Gaia will make a huge leap forward by providing accurate proper motions for a large fraction of the stars in the Milky Way, and several nearby ultra-faint dwarf galaxies [Antoja et al. 2015]. It will however struggle with more distant galaxies, when too large a fraction of their stellar population is below the detection threshold. HST proper motion studies have been carried out in the Local Group [e.g. LMC at 50kpc, Kallivayalil et al. 2013; Sagittarius stream at ~20kpc, Sohn et al. 2015; M31, at ~750kpc, Sohn et al. 2012]. However these studies are not accurate enough to trace internal proper motions from the individual stars. Nonetheless, the LMC result revolutionised our understanding of the relation between the Milky Way and the Magellanic Clouds by explicitly measuring their relative motions, which were not what was expected. MICADO will extend astrometry beyond the limits of HST and Gaia, to determine the detailed dynamical properties of the outer halo of the Milky Way and the Local Group.

With sufficiently accurate astrometry of a large number of stars in different stellar systems it is also possible to measure the internal variations in the velocities of individual stars, the velocity dispersion, in addition to their bulk motion across the sky. MICADO will be able to measure accurate density distributions and proper motions of faint stars near the centre of individual globular clusters and dwarf galaxies, much fainter than is currently possible. This will reveal the mass distribution within the system, and also indicate whether low/intermediate mass black holes are present and to what level globular clusters are actually as dark matter free as is currently thought. This will accurately define the range of mass over which black holes exist in the centres of stellar systems. Measuring the overall dark matter content of dwarf spheroidal galaxies our to the faintest stars in the outer regions is an interesting test of galaxy scale structure formation models. The internal proper motions of individual stars in dwarf spheroidal galaxies also reveals the mass and shape of the gravitational potential, which allow an accurate estimate of the amount and distribution of dark matter in these objects, and even possibly to set constraints on the physical nature of dark matter particles. Internal PMs can also directly measure the rotation of a stellar system.

Proper motions of individual stars in relatively distant stellar systems are very challenging measurements for a ground-based telescope. They require exquisitely detailed measurements of the positions of individual stars, to be able to track how they move in the plane of the sky over the timeframe of several years. This requires accurate relative astrometry over this time frame, which requires a very stable instrument and the ability to construct an accurate (local) astrometric reference frame using background objects like QSOs and galaxies that do not move. The higher the precision with which the measurements of the positions of individual objects can be made the more accurately the bulk motion and an orbital path determined. GAIA will do this for a substantial fraction of individual stars within the Milky Way, and in some cases up to 150kpc beyond. MICADO will have the power to push these kinds of detailed astrometric measurements to fainter stars and more crowded regions, and thus to the centres of dense nearby stellar systems and to more distant systems. With MICADO we can hope to obtain a detailed measurement of the dark matter mass and distribution beyond the Milky Way, to include the entire Local Group.

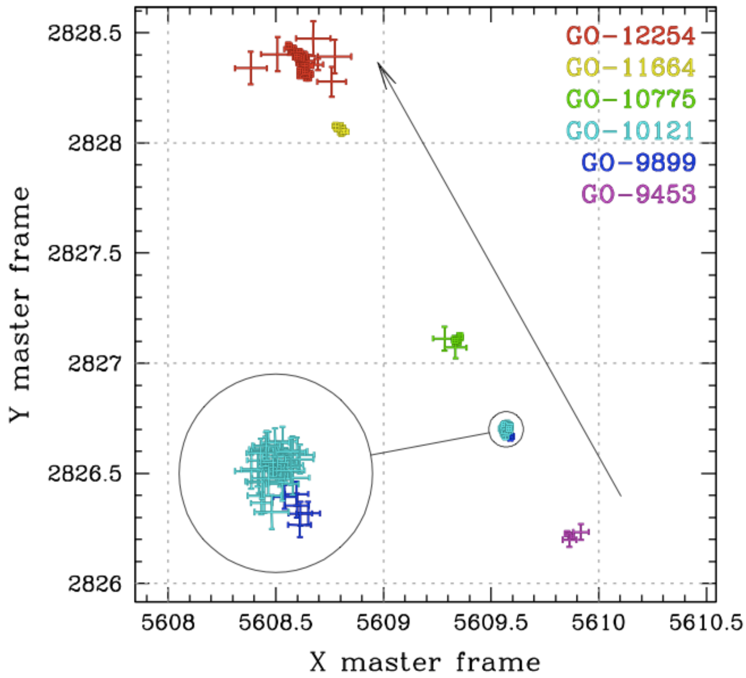

Figure 5.1: *The positions of a single star in globular cluster NGC6752, measured over 6 HST epochs as they appear in the reference frame. Star positions and error bars are colour coded according to the programme ID. The colours go from violet to green to red, moving from 2002 to 2006 to 2011 epochs. The black arrow shows the motion of the star over the 9 years of monitoring observations. The size of the error bars is related to the S/N of the measurements (some are short integrations). From Bellini et al. (2014).*

5.2 Importance of MICADO

Proper motions of individual stars measured in an image can distinguish the variety, and the kinematic properties of stellar systems overlapping in the photometric properties of the image (see Figure 5.2). The stars within each independent system will move in the same way. The systemic velocity dispersion can be measured from the size of the internal motions about the mean motion of the system. This is a very powerful way of removing fore- and background contaminating sources that move quite differently (see Figure 5.2); it can unveil the presence of otherwise undetectable tidal distortions or streams. If there is a large difference in velocity between members and contaminants, this does not require exceptional precision. However to go one step further and interpret the details of the motions of the individual stars in each distinct population (e.g. measuring the velocity dispersion) requires considerably more care and the precision has to be at least smaller than the systemic velocity dispersion. Also, to obtain absolute proper motions this requires the local reference system to be anchored to an absolute reference (e.g. distant quasars or galaxies in the field).

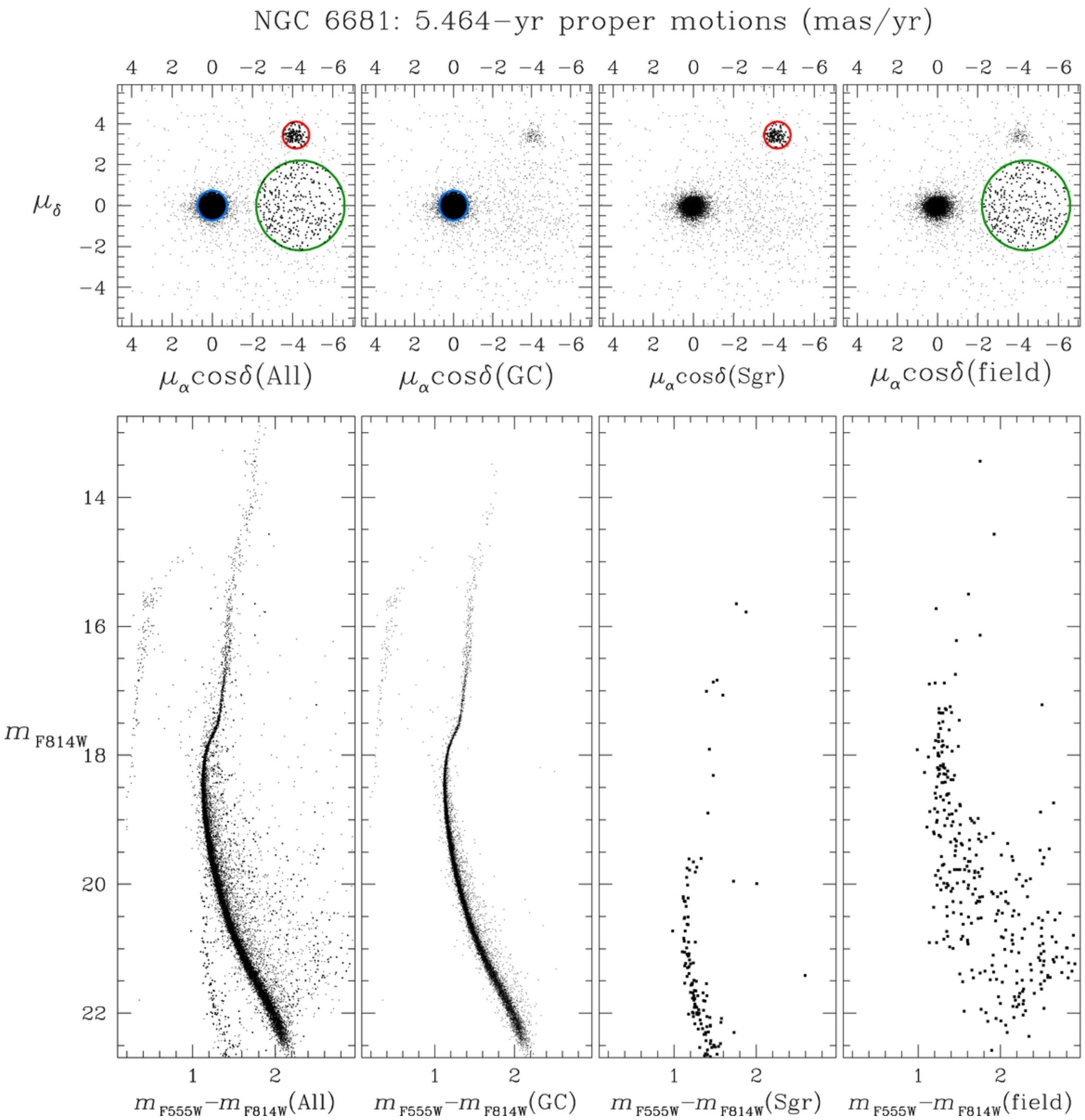

Figure 5.2: *The upper panels show the vector point diagrams of the relative proper motions of all the stars in the HST field of the globular cluster NGC6681. In the lower panels, the CMDs corresponding to the selections applied in the upper plots are displayed. First column: the full colour-magnitude diagram of the field, no selection is applied. Second column: the cluster members are selected within the blue circle and the corresponding CMD displays only well-defined cluster evolutionary sequences. Third column: Sgr dSph selection within the red circle and corresponding CMD. Fourth column: the selection of the bulk-motion of field stars and their location on the CMD.*

HST accuracy and stability for astrometry is well documented, and assuming appropriate software and properly sampled images it has been shown that an astrometric precision <1% diffraction limit is possible (e.g., Bellini et al. 2014; Massari et al. 2013), see Figure 5.2. A similar level of accuracy has also been achieved on ground based images (<1% the seeing disc), which this is 7mas, or 0.03 pixels for the WFI@2.2m, corresponding to ~0.75% FWHM [Anderson et al. 2006]. It has also been shown that the SCAO assisted NACO@VLT can reach an astrometric precision of 200µas, i.e., ~0.50% DL @1.2µm [REF]. Looking at the MCAO instrument GeMS on Gemini an astrometric precision of 500 µas (<1% DL) found @2.1µm [Massari et al. 2016]. Assuming MICADO can achieve a similar level of accuracy this should enable **unprecedented diffraction-limited position measurements of 40µas a single image**. However if it is possible to control the systematics, in principle this precision should scale with 1/sqrt(N), where N is the total number of images over which the astrometric precision is reached. Optimistically it should then be possible to achieve a precision (with multiple images) down to <10µas [Cameron et al. 2009]. Over a time baseline of 10 years, we may therefore hope to reach a proper motion accuracy of about 2µas/yr. Note that these numbers refer to relative motions of nearby objects on the same exposures; on larger scales these accuracies can only be attained provided an accurate astrometric reference frame can be established. A similar precision in relative parallax measurements should be attainable.

For comparison, GAIA is predicted to deliver proper motion accuracies as low as 4 µas/yr, over a five-year mission lifetime. However this precision will only be reached for very bright stars (V<10). At V=15(20), the error is expected to be 5-15(100-300) µas/yr.

MICADO will be able to measure proper motions with an accuracy of more than an order of magnitude greater than HST, and at much fainter magnitudes. In fact, after only five years it will be possible to reach 10µas/yr, which is equivalent to a motion of 5km/s at 100- [Trippe et al. 2010]. At this level, many novel science cases become feasible, including proper motions of stars in the centre of our Galaxy and also other nearby galaxies; mass determinations of intermediate mass black holes; proper motions of globular clusters and their multiple populations, and testing cold dark matter structure formation from the internal kinematics of dwarf spheroidal galaxies. MICADO will be perfectly complementary to GAIA for proper motion measurements of faint objects, and/or for highly reddened or crowded environments, and a number of interesting science cases can be foreseen.

Looking for intermediate black holes: With this level of precision, an intriguing science case is the hunt for intermediate mass black holes in the centre of stellar clusters and also nearby low mass dwarf galaxies. These are black holes with masses intermediate between stellar mass (M<20 $M_\odot$) and super massive ($M>10^6 M_\odot$) found in the centres of large galaxies. By simply following the M_host-M_BH Magorrian relation, one of the most promising places to find them is the centre of star clusters, where theory predicts several mechanisms by which they may have formed. However, to date no conclusive evidence has been found of their existence. A major obstacle to overcome in this search is the extreme stellar crowding in the inner regions of dense clusters, which makes very difficult to properly perform photometric (a cusp in the density profile can be a signature of the presence of an IMBH) and kinematic (the tell-tale signature of an IMBH is a cusp in the velocity dispersion profile) studies. The superior resolution of MICADO will make it possible to solve this problem, at least for Galactic clusters and close satellites.

Cluster parallaxes: For parallax measurements, we need to consider the following reference number: at 1kpc we have a parallax semi-displacement of 1.0mas. Accounting for multiple images, and most importantly, for the fact that we can measure the parallax of a large number of stars, we expect to measure parallaxes of star clusters and stellar agglomerates at least out to the distance of the LMC with errors significantly smaller than 10%, i.e. for all of the Galactic star clusters, in particular those heavily obscured or in a crowded environments, which are not measurable by GAIA. Distances accurate to better than10% are a pre-requisite for obtaining cluster ages to better than 20%, and because distance is necessary to compute the orbit, a small distance error translates into more accurate orbits/orbital history.

Internal motion and rotation of resolved stellar systems: With a typical internal velocity dispersion of 5km/s the proper motion dispersion is 100 µas/yr at 10kpc, hence one can measure an internal proper motion field with errors significantly less than 10% in a few years out to a few tens of kpc. The only limiting factor for internal tangential motion is the number of measured stars. Combined with radial velocities and orbit models, such measurements can also be used to derive distances.

Absolute Motions of GCs and dwarf galaxies: The Proper motion precision on a single high S/N point source in 5 years is 10μas/yr, and better if combined with HST archive data. At 10kpc, 50km/s corresponds to 1000μas/yr, i.e. one single absolute reference source would allow a 1% precision in the absolute proper motion measurement. At 100kpc, 200km/s corresponds to 400μas/yr, i.e. one single point like reference source would allow a 2.5% precision. See Figure 5.3. The problem may be the lack of absolute point sources (e.g. QSOs) in a single MICADO frame. In that case we can use many faint high-redshift galaxies, in particular taking advantage of quasi-point like sources within each of them. In this case one would need to reach galaxies at very faint magnitudes. Globular cluster astrometry using faint galaxies for the astrometric reference has been successfully achieved with HST [Kalirai et al. 2007]. Thus, obtaining the full 3D motion of virtually all Galactic globular clusters should to be feasible with MICADO@EELT, and it can look at the dwarf spheroidal and ultra faint dwarf galaxies around the Milky Way. I am not sure how this compares to GAIA/HST ongoing work [DM:I am checking this with Amina. Gaia will measure PMs for a sufficient number of stars out to about 100-150 kpc. Whenever a HST 1st epoch exist, it should be possible to measure the absolute PM. This means that using Gaia as 1st epoch, MICADO will be able to measure the PMs of all the newly discovered dwarfs/ultra faints and stellar streams that lack HST measurement.]

Such measurements constitute a test to what extent these satellites have been accreted following a preferential direction, as suggested by the possible discovery of a common plane both in the MW (the so called vas polar structure, e.g. Pawlowski et al.13) and in M31 (Ibata et al. 2013)]

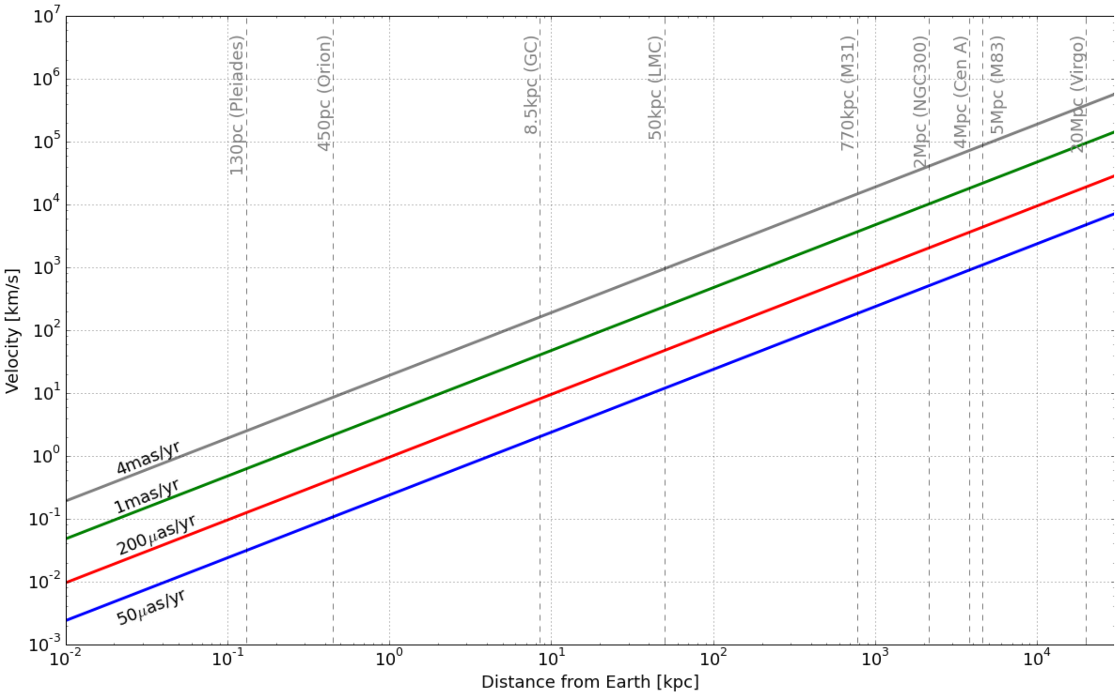

Figure 5.3: *How the proper motion traces the velocity of a system with increasing distance.*

Binaries in globular cluster cores: With 50 μas resolution one can measure the wobble of all binary members with a dark companion (black hole, neutron star, white dwarf) with a mass > 0.5$M_\odot$ and separation > 0.5AU in globular cluster out to 10kpc. The numbers scale accordingly for more distant clusters. Binaries for which both components are visible are harder to measure, but feasible. The same observations would allow one to study the proper motion of stars very close to the cluster center, and therefore explore the presence of IMBH for clusters well beyond 10kpc.

Dark matter in dwarf galaxies: Measuring the dark matter content of dwarf galaxies around the Milky Way and beyond is a fundamental test of structure formation models. CDM simulations of gravitational collapse show that extended halos like that of the Milky Way and the Local group should be highly structured, with numerous clumps, as a consequence of hierarchical merging. On the assumption that these clumps (sub-halos) host stellar populations, the visible mass function of the satellites should be similar to what is seen in the (dark matter) simulations. It is important to robustly establish if this relation is consistent with observations. If it is not observed, then this would require a significant modification in the CDM structure formation mechanism, or the way that baryons evolve within dark matter halos, where they may be disrupted by early star formation and mass loss (feedback) processes.

There has been significant observational effort in this area with large spectroscopic surveys measuring line-of-sight radial velocities of individual red giant branch stars in nearby resolved galaxies, to measure their dynamical masses using velocity dispersion profiles. Typically, the measured velocity dispersions stay flat out to large radii, suggesting that the dwarf spheroidal satellites are surrounded by massive halos. However these radial-velocity measurements are subject to orbit anisotropy degeneracy, meaning that a deeper potential can mimic a tangentially biased orbit distribution. Proper motions are the only way to break this degeneracy, as this makes it possible to directly measure the shape of the velocity ellipsoid (ratio of the radial and tangential velocity dispersions) of the stars. It has been shown that adding proper motion information for samples as small as 160 stars, it is possible to obtain accurate estimates of both the velocity anisotropy and mass slope, and thereby unambiguously break model degeneracies [Wilkinson et al., 2002]. This is also confirmed by Strigari et al. (2007), who show that, for general dark matter density and anisotropy profiles, the log slope of the dark matter profile at about 2 core radii can be measured to within ±0.2 if the proper motions of 200 stars (with tangential velocity errors of ~5 km/s) are added to the line of sight velocity measurements. This would allow tighter constraints on the type of dark matter halos hosting dSphs, and hence possibly also on the nature of dark matter.

Given the internal velocity dispersions of ~10km/s for these objects, MICADO will be able to measure these internal motions securely from a five-year baseline for objects as distant as 100kpc (10km/s/100kpc corresponds to 21μas/yr). This accuracy is more than sufficient to measure the shape of the velocity ellipsoid in the more nearby systems. Much more dynamical information, such as the relaxation level of the systems, detailed distribution functions, behaviour at the tidal radius, etc., can be obtained by combining a proper motion survey with radial velocity measurements of the same stars.

These bulk-motion measurements can also be used to derive orbits of the satellites systems in the galactic potential, assuming that an external reference frame can be established with background QSOs or galaxies in the field. The internal motions of dwarf spheroidal galaxies reveal the gravitational fields in these systems

References:

Antoja T. et al. 2015 MNRAS, 453, 541; Bellini A. et al. 2014 ApJ, 797, 115; Battaglia G. et al. 2005 MNRAS, 364, 433; Battaglia G. et al. 2008 MNRAS, 383, 183; Cameron P.B. et al. 2009 AJ, 137, 83; Harris W.B. 1996 AJ, 112, 1487; Ibata R. et al. 2013 Nature, 493, 62; Kalirai J. et al. 2007 ApJL, 657, 93; Kallivayalil N. et al. 2013 ApJ, 764, 161; Massari D. et al. 2013 ApJ, 779, 81; Massari D. et al. 2016 A&A Lett, 595, 2; Mateo M. 1998 ARAA, 36, 435; McConnachie A. 2012 AJ, 144,4; Pawlowski M.S. et al. 2013 MNRAS, 435, 1928; Sohn S.T. et al. 2012 ApJ, 753,7; Sohn S.T. et al. 2015 ApJ, 803, 56; Strigari L.E. et al. 2007 ApJ, 669, 676; Tolstoy E. et al. 2004 ApJL, 617, L119; Trippe S. 2010 MNRAS, 402, 1126; Vera-Ciro & Helmi 2013 ApJL, 773, 4; Walker M. et al. 2009 ApJ, 704, 1274; Wilkinson M. et al. 2002 MNRAS, 330, 778

6. Resolved stellar populations

Text from Phase A study, adapted by E. Tolstoy 31/10/2016
Coordinator: Eline Tolstoy (NOVA/Groningen)
Contributors: S. Larsen, N. Przybilla, S. Sietz, João Alves, Kieran Leschinski
Technical Templates: A.12, A.13, A.14, A.15, A.16 (Imaging); A.17, A.18 (Spectroscopy)

6.1 Outstanding Questions

One of the key issues in modern astrophysics concerns the star formation history (SFH) of the Universe; where and when have most stars formed. This is of critical importance to understand the link between cosmological dark matter evolution and the visible baryonic matter that we can directly observe. The development of large structures in the Universe can be successfully explained in terms of hierarchical growth in the framework of a Lambda Cold Dark Matter (ΛCDM) model, however it is still not clear how to couple the baryonic component to the dark matter. Direct observations of galaxies up to high redshift can be used to map the current star formation rate and how it changes with look-back time, but since the integrated galaxy light is dominated by the most recent stellar generations, the information on the underlying older stellar population is limited. A similar problem affects the analysis of the spectral energy distribution of galaxies, from which only luminosity averaged ages and metallicities can be derived.

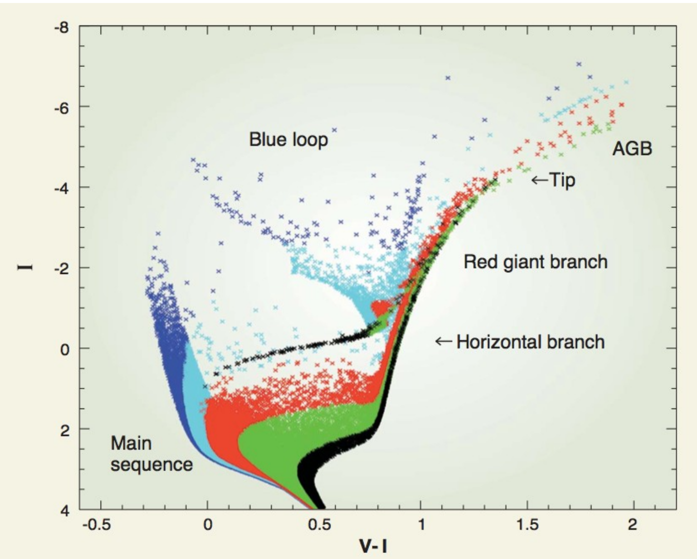

Figure 6.1: *A simulation, from stellar evolution models, of a Colour-Magnitude Diagram, for a galaxy that has constantly formed stars over the last 13 Gyr. The stars are colour-coded according to age: blue, stars <300 Myr old; cyan, 0.3 to 1.1 Gyr; red, 1.1 to 3 Gyr; green, 3 to 8 Gyr; black, >8 Gyr. Key stellar evolution phases that clearly mark the presence of stellar populations of different ages are labelled. The red giant branch is clearly a poor age discriminator, whereas on the main sequence the different age groups are distinct. The horizontal branch contains stars >10 Gyr old and is thus an unequivocal indicator of the presence of an ancient stellar population. From Tolstoy (2011).*

It is only by resolving individual stars and accurately putting them in a Colour-Magnitude Diagram (CMD) that galaxy evolution, the star formation rate versus time, can be accurately measured to trace the fossil record of the SFH back to the early Universe. This has been impossible for the central regions of giant galaxies because of crowding and sensitivity limits, but it is here that the majority of ancient stars are to be found, and thus the most detailed information about galaxy origins. MICADO will make it possible to resolve individual ancient these stellar populations in the heart of giant galaxies outside the Local Group. This will dramatically improve the detail and accuracy of comparisons between observations of galaxy evolution going back to the oldest stars that formed in the early Universe and simulations that start in the early Universe and predict present day galaxy properties. The detailed analysis of the properties of ancient stars is possible because low-mass stars have very long lives, and in many cases their photospheres remain untouched samples of the gas out of which the star formed. When ancient low mass stars can be individually identified they provide uniquely accurate probes of the detailed physical conditions in the early Universe when galaxies were assembling. Stars of different ages thus can be used to follow galactic scale evolution, as the rate at which stars form in a galaxy with time is a direct measure of how the global properties (e.g. luminosity, colour, mass) change. This can only be uniquely determined by careful CMD analysis (e.g. see Figure 6.1).

At present, ancient resolved stellar populations can only be uniquely identified in the Milky Way and the closest of our neighbouring galaxies, which are predominantly small dwarf galaxies [Mateo 1998; Tolstoy, Hill & Tosi 2009]. To make a breakthrough in our understanding of galaxy formation and evolution we need to study ancient stars and make accurate star formation histories in different environments and most importantly in massive galaxies, which contain the bulk of the stellar mass in the Universe. This means in the bulges and discs of Spiral galaxies (e.g. in the Sculptor group at 2- 3Mpc); S0 galaxies; and Elliptical galaxies in a cluster environment, like in Virgo (16-18Mpc), see Figure 6.2. These are all key objects to study the star formation history of the Universe [e.g. Madau & Dickinson 2014]. The current limitations in extending these studies to greater distances are both sensitivity and spatial resolution. The oldest Main Sequence Turnoff stars in a CMD are the most reliable age indicators (see Figure 6.1), but this requires accurate photometry at m_I~28 at 1Mpc distance. This is possible with the Hubble Space Telescope (HST) only with very long exposures, and only for very low surface brightness dwarf galaxies due to crowding and sensitivity limits [e.g. Cole et al. 2007]. It will also be challenging with JWST for similar reasons.

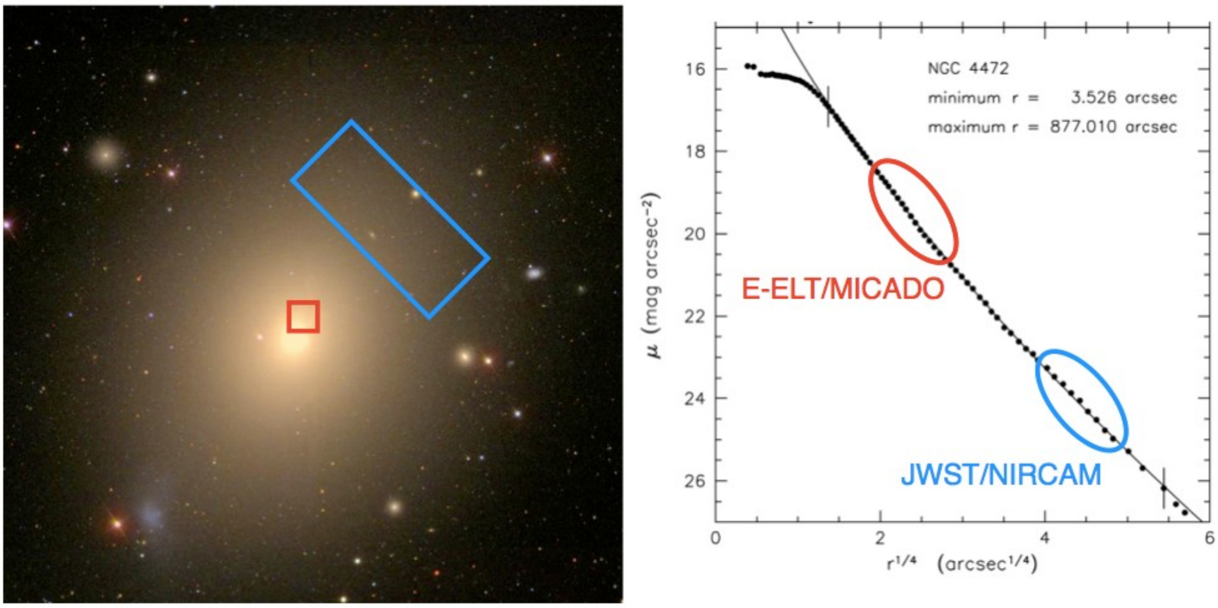

Figure 6.2: (left) *An image of NGC4472 (M49), an Elliptical galaxy in the Virgo cluster, with possible areas that could be surveyed by JWST, blue rectangle and MICADO, red square.* ***(right)*** *The surface brightness profile of NGC4472 is shown to show where individual red giant branch stars can be resolved with both MICADO and JWST, clearly in different regions of the galaxy.*

In short, we have a compelling theory of galaxy formation and evolution [e.g. Springel et al. 2005; Schaye et al. 2015], but observational verification on the scale of individual galaxies is challenging to interpret for a variety of reasons, and the results of these comparisons often appear contradictory [e.g., Moore et al. 1999; McGaugh et al. 2000; Tolstoy et al. 2003; Venn et al. 2004; Boylan-Kolchin et al. 2012]. A major issue that MICADO will tackle is that we have very little direct proof of the major merger history of large galaxies. The Milky Way is a single galaxy that we can study in this detail and there is little direct evidence for this, but it may have led a quiet life. M31 is also open for study buts proximity to the Milky Way makes this something of a challenge, and two spiral galaxies are hard to argue as a good sample of large galaxies in the Universe. An exciting possibility that becomes feasible with MICADO is to combine deep CMD analyses of the bulges of a sample of nearby Spiral galaxies, and the central regions (within the half light radii) of Elliptical galaxies with proper motions, spectroscopic radial velocity measurements and chemical abundance measurements, as it has been done for dwarf galaxies in the Local Group [e.g. Tolstoy, Hill & Tosi 2009; Tolstoy 2011]. This will provide extremely detailed information to compare with predictions from simulations. Photometry and astrometry in high surface brightness crowded stellar fields beyond the Local Group requires MICADO on the E-ELT. These have long been science drivers for the E-ELT [Hook 2005].

6.2 Importance of MICADO

Star formation histories beyond the Local Group: Only by resolving individual stars in a galaxy and carrying out accurate photometry in at least two filters is it possible to uniquely determine the star formation history and the accompanying chemical evolution pathway of a galaxy [e.g. Tosi et al. 1991; Tolstoy & Saha 1996; Dolphin 2002; Aparicio & Hidalgo 2009; de Boer et al. 2012]. The major observational challenge is that low mass ancient stars are faint, and they are often severely crowded together. This means that their study requires the demanding combination of high spatial resolution, flux sensitivity and also a high dynamic range (of order 10 magnitudes), see Figure 6.1.

Stellar age dating is most effective at the Main Sequence Turn-off region, but additional information can also be gained from Horizontal Branch stars (Salaris et al. 2013), and also from the intrinsically brightest regions of the CMD for recent star formation (Dohm-Palmer et al. 1997). Old stellar populations can be uniformly sampled on the Red Giant Branch, as can be seen in Figure 6.1. This figure also shows that old main sequence stars in galaxies can quickly become prohibitively faint even for MICADO, while accurate photometry of bright RGB stars will be feasible out to the Fornax Cluster and beyond (Deep et al. 2011; Greggio et al. 2012).

HST, with its high spatial resolution and sensitivity, and uniquely stable Point Spread Function, led to a breakthrough in the study of resolved stellar populations in Local Group dwarf galaxies [e.g., Dohm-Palmer et al. 1997; Tolstoy et al. 1998; Tosi et al. 2007; Cole et al. 2007; Tolstoy, Hill & Tosi 2009; Weisz et al. 2014]. However, the small 2.4m diameter of HST struggles with both sensitivity and spatial resolution for galaxies beyond ~1Mpc, see Figure 6.3, and thus we need to expand these capabilities for another breakthrough by pushing our vision beyond the Local Group into different environments, with more giant galaxies. JWST should improve on HST performance for both sensitivity and spatial resolution, but MICADO will provide the necessary leap to push this kind of analysis well beyond the Local Group and deep into the heart of giant galaxies.

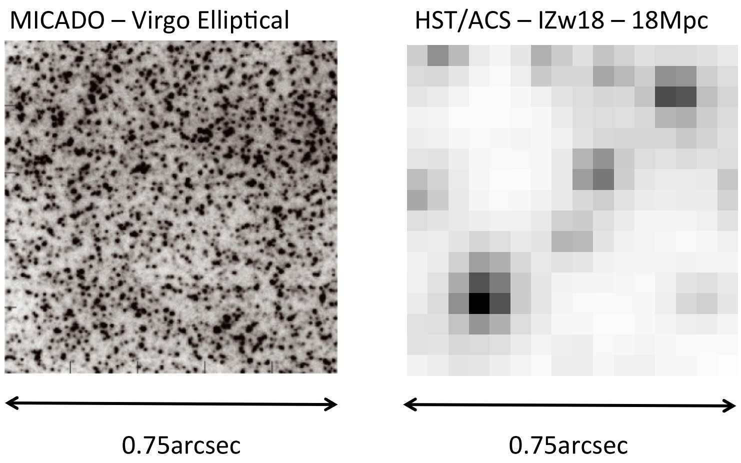

Figure 6.3:* *(left) *A simulated I-filter image of a field at a surface brightness of 19mag/arcsec^2 in an Elliptical galaxy in Virgo at 18 Mpc distance, from Deep et al. 2011. The stars in this image are mostly red giant branch stars.* ***(right)*** *An observed I-filter image taken over a similar area at a similar surface brightness from a deep HST/ACS pointing near the centre of the star-forming blue compact dwarf galaxy IZw18, which is also at 18 Mpc distance. The stars in this image are all supergiants and the fainter background population is not resolved.*

Potential targets start with large spiral galaxies at the edge of the Local Group, such as NGC3109 (at 1.4Mpc) and NGC55 (at 1.9Mpc), which are small spiral galaxies. In addition there are 3 medium-sized spiral galaxies in the Sculptor group (NGC253, NGC300 and NGC247), one of which is a starburst. The Sculptor group also contains a number of large and small irregular galaxies, and observing these will give us a detailed comparison to the similar galaxies in the Local Group. But the unique application for MICADO that will not be possible with any other facility is to look deep into the high surface brightness centres of Spiral galaxy bulges and Elliptical galaxies. The nearest by Ellipticals, after the peculiar more S0 like system Centaurus A, are in clusters such as Virgo (at 18Mpc distance) and Fornax (at 19Mpc).

Observing Star Formation in different environments: Star formation and how its properties vary with environment remains a challenging field. Measuring the properties of low mass star formation, and thus the form of the Initial Mass Function (IMF) is a critical element in this study. It requires accurate photometry in crowded regions down to faint magnitudes and thus MICADO can make a major contribution especially in pushing these detailed studies into a wide range of environments beyond the Milky Way. An important aspect is to connect the gas properties with the star formation rate (SFR).

There have been numerous recent efforts to develop and refine theories behind all aspects of star formation, and yet we still do not have a predictive theory of star formation and realistic star formation models are critically needed for understanding almost every process in the universe, from the evolution of galaxies to the formation of planetary systems.

Galaxy evolution models rely on an accurate IMF and SFR to describe their feedback mechanisms. Determining the star formation history of a galaxy is impossible without assuming an IMF and an SFR [Madau et al. 1998, Kennicutt 1998]. At the other end of the scale, the dynamics of the interstellar medium (ISM) and planet formation require an intimate knowledge of the chemistry of the universe, for which we need information on how, where, when, which, and how stars are formed.

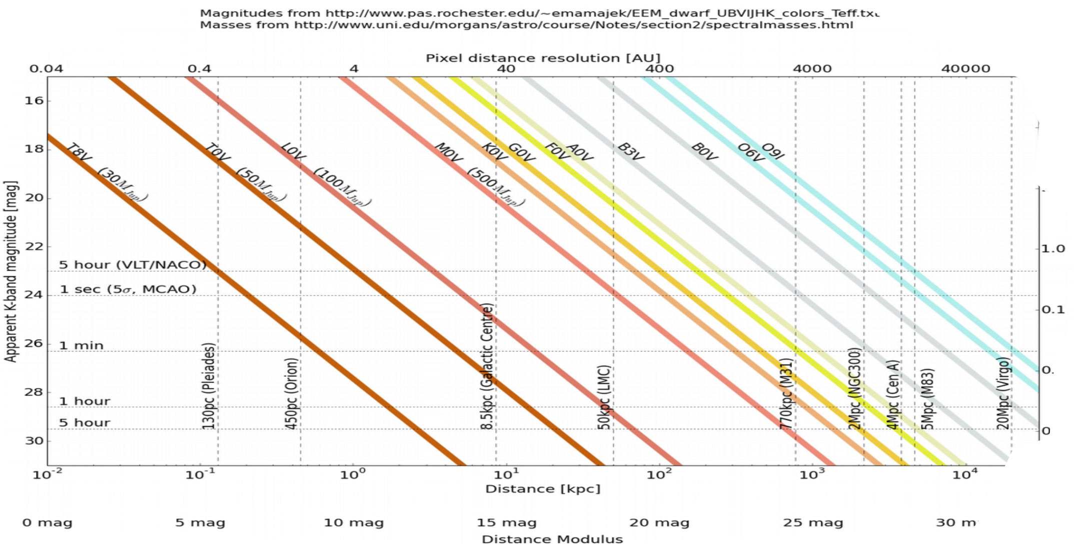

Figure 6.3: *Sensitivity-distance parameter space for resolved stars with MICADO.*

Currently, resolved observations of these aspects of star formation, or some of them, are limited to the Milky Way and the Magellanic clouds. Only the large increase in both sensitivity and angular resolution in the near-infrared (NIR) regime that the Extremely Large Telescope and MICADO will provide, will finally allow us to peer into the realms of resolved star formation in many of the other galaxies in the Local Group, see Figure 6.3 for the effect of distance and resolution on our ability to resolved individual stars of different types (and thus luminosities)

Cepheid period-luminosity relation out to 100Mpc: The Hubble constant estimates from the Planck Satellite and from local Cepheids & Supernovae (SN) are both formally precise but also to some degree in conflict with each other. If confirmed this would indicate deviations from the cosmological standard model. For a definite conclusion it is necessary to further decrease the error of the local Hubble constant estimate and to understand better the systematics. Such a more precise H0 measurement is of general interest since it also decreases the errors on the time derivative of the dark energy equation of state measurements in cosmological surveys.

The local Hubble constant is measured using the distances to SN-host galaxies based on the period-luminosity-relation (PLR) of Cepheids (Reiss et al. 2011). The error for H0 is estimated to be 3 percent when LMC and Milky Way Cepheid parallaxes and the maser distance to NGC 4258 are used. The high precision was obtained by measuring near infrared PLRs with HST, which are less sensitive to metallicity and to extinction in the host galaxies, benefiting from the photometric accuracy and stability of HST.

Decreasing the H0 error requires many more Milky Way Cepheids with parallax distances and increasing the "local" SN-host galaxy sample (to at least 80). The last point assumes that PLR relations to more distant SN hosts can be measured as well. Because of the increased stellar crowding this will be beyond HST and requires instruments with a better spatial sampling, like MICADO. MICADO outperforms JWST and is the ideal instrument to push Cepheid PLR estimates to 100 Mpc (Coma cluster), and thus to galaxies participating in the Hubble flow. The stability (spatially and in time) and a well understood form of the PSF has to be ensured in order to relate the fluxes in the core of the Cepheids to the entire PSF-fluxes. These data should allow photometry with biases not exceeding the 1 percent level.

Ca II triplet spectroscopy beyond the Local Group: The detailed spectroscopic study of individual stars in nearby galaxies allows the determination of accurate metallicity distributions and kinematic properties for stars of a range of age in a range of different nearby galaxies. One common method that has been well calibrated for red giant branch (RGB) stars, uses intermediate resolution spectroscopy of the Ca II triplet (CaT) metallicity indicator. With an R~8000, it can provide accurate line-of-sight velocities (±1–2 km/s) and metallicities ([Fe/H], ±0.1–0.2 dex) from the equivalent widths (EW) of CaT lines (e.g. Battaglia et al. 2008a; Starkenburg et al. 2010). RGB have ages from > 1 Gyr to the age of the Universe, and are thus tracers of all but the most recent star formation processes in a galaxy. At the present time to even get much beyond the outer halo of the Milky Way is challenging, and requires long exposures with sensitive multi-object spectrographs on the largest telescopes (e.g., FORS/VLT, FLAMES/VLT, Deimos/Keck, MIKE/Magellan). Hence the studies to date have been restricted exclusively to the nearest *dwarf* galaxies. Large numbers of careful measurements have led to a deeper understanding of the chemical evolution and also the dynamical state of these systems.

Naturally the next step in this field is to extend these studies, using the same well established and calibrated methods, to a broader range of galaxy types. This requires us to look beyond the Milky Way halo and even the Local Group. With MICADO we can look beyond the Local Group, to the Sculptor group, for example, which contains a range of different galaxy types (from large spiral galaxies to small gas rich and gas poor dwarf galaxies) and allows us to study a different group environment in detail. Finally the ultimate goal is to be able to make a study of the resolved stellar populations in giant elliptical galaxies, of which there is no example in the Local Group, and we have to look at Cen A (at 4 Mpc) to find the closest example, of a peculiar elliptical. These CaT spectra allows us to probe the total mass of these galaxies and also the chemical evolution history of all components (i.e., disk, bulge and halo), including a kinematic deconvolution of these components and a comparison of their detailed properties over a range of galaxy type and environment. We will also obtain a more accurate picture of the dark matter properties of a range of different galaxy types, the effects of tidal perturbation and the ubiquity of metallicity distribution functions.

Resolved versus unresolved stellar populations: As one pushes to more distant galaxies the brighter stars are resolved and the fainter stars are hidden in the crowded background. This gives the interesting possibility of analyzing semi-resolved stellar populations. Using the bright stars to predict the underlying stellar component corresponding to the bright stars and analyzing the properties of the unresolved population to see what is missing. This could allow relatively detailed SFHs of more distant galaxies than is currently possible. However this does require that the method is calibrated on more fully resolved stellar systems to ensure the accuracy and efficacy of the method is properly understood.

References:

Aparicio A. & Hidalgo S. 2009 AJ, 138, 558; Battaglia G. et al. 2008 ApJL, 681, L13; Boylan-Kolchin M. 2012 MNRAS, 422, 1203; Cole A.A. et al. 2007 ApJL, 659, L17; de Boer T.J.L. et al. 2012 A&A, 539, A103; Deep, A. et al. 2011 A&A, 531, A151; Dohm-Palmer R.C. et al. 1997 AJ, 114, 527; Dolphin A. 2002 MNRAS, 332, 91; Greggio L. et al. 2012 PASP, 124, 653; Hook I.M. (ed.) 2005 *The Science Case for the European Extremely Large Telescope;* Kennicutt R.C. 1998 ApJ, 498, 541; Madau P. et al. 1998 ApJ, 498, 106; Madau P. & Dickinson 2014 ARAA, 52, 415; Mateo M. 1998 ARAA, 36, 435; McGaugh S. et al. 2000 ApJL, 533, L99; Moore B. et al. 1999 ApJL, 524, 19; Salaris M. et al. 2013 A&A 559, A57; Schaye J. et al. 2015 MNRAS, 446, 521; Springel V. et al. 2005 Nature, 435, 629; Starkenburg E. et al. 2010 A&A, 513, A34; Tolstoy E. & Saha A. 1996 AJ, 462, 672; Tolstoy E. et al. 1998 AJ, 116, 1244; Tolstoy E. et al. 2003 AJ, 125, 707; Tolstoy E., Hill V. & Tosi M. 2009 ARAA, 47, 371; Tolstoy E. 2011 Science, 333, 176; Tosi M. et al. 1991 AJ, 102, 951; Tosi M. 2007 in *From Stars to Galaxies: Building the Pieces to Build Up the Universe*, *ASP Conf. Ser.*, 374:221; Venn K.A. et al. 2004 AJ, 128, 1177; Weisz D. et al. 2014 ApJ, 789, 147

7. Planets & Planet Formation

There was no reference to this in Phase A – new
Responsible: Anthony Boccaletti/ Gael Chauvin

Contributors:
Technical Templates: A.19 (Imaging)

7.1 Outstanding Questions

The observation and characterization of exoplanets and planetary architectures is crucial to expand and complete our view of planetary formation and evolution, as well as of the physics of exoplanets. With two decades of exoplanet studies, observations regularly obtained key successes with the discovery of the Hot-Jupiters family, the detection and confirmation of about 2000 exoplanets today (see http://exoplanet.eu), the first glimpse of planetary atmospheres and internal structures, the first images of exoplanets, the discovery of Super-Earths in the Habitable Zone (where water is expected to be liquid) or more recently Earth-mass or Mars-size planets. The five main hunting techniques currently used (radial velocity, transit, micro-lensing, direct imaging and astrometry) are complementary and can be combined to further constrain planet properties like density (using radial velocity and transit) or internal entropy (radial velocity and imaging). Radial velocity and transit surveys have been very successful with the discovery of thousands of planetary candidates. However, together with micro-lensing and astrometry, these techniques mainly enable a study the inner parts of exoplanetary systems, at less than 5–10 AU (see Figure 7.1). Direct Imaging (DI) is uniquely able to explore the outer parts at more than 5-10 AU to complete our view of exoplanetary system architectures. In addition to the orbital properties, the exoplanet's photons can be resolved and dispersed to spectroscopically probe the atmospheric properties of the imaged exoplanets. As mostly young exoplanets are discovered as they are hotter and brighter when young, the study of their atmospheres show low-gravity features, as well as the presence of clouds, and the non-equilibrium chemistry processes. Moreover, DI enables a direct probe of the presence of planets in their birth environment. Their physical properties can then be directly connected to the observed spatial structures in young proto-planetary or debris disks to study the planet – disk interactions and stability of the system.

Figure 7.1: *Exoplanet discoveries in May 2015 for the different planet hunting techniquse. The exoplanet masses are shown as a function of their distances to the host star.*

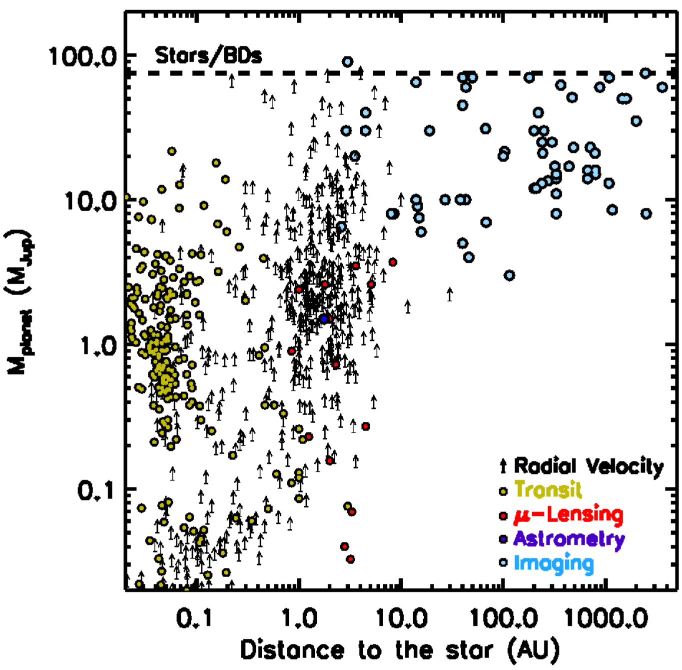

In the upcoming decade, the perspective is rich in terms of space missions and ground-based instrumentation dedicated to the field of exoplanet detection and characterization. Following the new generation of planet imagers fully dedicated to the research and the characterization of exoplanets SPHERE and GPI, the

VISIR+, ERIS and MATISSE spectro-imagers will offer a complementary view in mid-infrared. At sub-mm and centimetre wavelengths; ALMA in full capability will pursue the characterization of the cold dusty and gaseous component of young protoplanetary and debris disks with an exquisite spatial resolution (down to 0.1”) completed by the Square-Kilometer Array (SKA) starting in 2020. The arrival of a new generation of high-resolution spectrographs CRIRES+, ESPRESSO at VLT, SPIROU at CFHT and NIRPS at the ESO3.6m Telescope will extend the current HARPS horizon to the population of light telluric planets around solar and low-mass stars (Mégevand et al. 2012). In space, Gaia, launched end-2013, will achieve a final astrometric precision of 10 µas in the context of a systematic survey of a billion of stars and therefore discover thousands of new planetary systems. Gaia should give us a complete census of the giant planet population between 2 and 4 AU for stars closer than 200 pc (Sozzetti et al. 2011). The new transiting exoplanet survey satellite (TESS, Transiting Exoplanet Survey Satellite, launch date 2017, Ricker et al. 2010) will go beyond the Corot and Kepler missions. It is designed for a full-sky survey to reveal thousands of transiting exoplanet candidates with the size of Earth or larger and orbital periods of up to two months. This will be complemented by the CHEOPS (CHaracterising ExOPlanet Satellite) mission aimed at characterizing the structure of exoplanets with typical sizes ranging from Neptune down to Earth diameters orbiting bright stars (launch date in 2017). Finally, PLATO (Planetary Transits and Oscillations of Stars), foreseen for 2024, will extend our knowledge on the content of telluric planets at longer periods, up to several years, around relatively bright, nearby stars. Within 10–15 years, the era of large-scale systematics surveys will end thanks to a complete census of exoplanetary systems within 100–200 pc from the Sun. They will be completely devoted to the population of telluric planets.

Thus, a new era is about to begin, fully dedicated to the characterization of known systems. Hubble, Spitzer and the first generation of planet imagers and spectrographs on 8m ground-based telescopes have already initiated these studies. The characterization of the physics of giant planets will intensify with the operation of the James Webb Space Telescope (JWST), foreseen for the year 2018, which will address several key questions for the study of young circumstellar disks and exoplanetary atmospheres using direct imaging and transit and secondary eclipse spectroscopy (Clampin and Smith, 2010). Despite a reduced sensitivity compared to JWST, the new generation of extremely large telescope, the Giant Magellan Telescope (GMT; Shectman and Johns 2010), the Thirty Meters Telecope (TMT; Simard and Crampton 2010) and the European Extremely Large Telescope (hereafter EELT; McPherson et al. 2012), will offer a unique spatial resolution and instrumentation. With the First Light foreseen in 2024-2026, the EELT will arrive at a propitious time to exploit discoveries of the upcoming generation of instruments and space missions owing to its capabilities in terms of sensitivity, spatial resolution and instrumental versatility. In this context, MICADO offers the possibility to image and characterize planets and young planetary systems at the EELT diffraction limit in near-infrared (10mas at K-band). The high-contrast imaging mode of MICADO will use the combination of SCAO-correction, coronography and angular differential imaging to bring us a step further with the E-ELT at 1st Light to address several outstanding questions still unanswered:

1 How do giant planets form? Understanding how the giant exoplanets form, how they evolve and interact, is critical because they completely shape the planetary system architecture and offer the possibility to form Earth or Super-Earth-like planets, i.e. rocky planets on a stable orbit sustaining Life. Nowadays, there are still fundamental questions that are unanswered. We do not know if there is one formation mechanism or several mechanisms to form giant planets and possibly operating at different timescales, locations and physical conditions. We do not understand the influence of the initial conditions, i.e. the impact of the stellar mass, the stellar metallicity and multiplicity or the effect of the close stellar environment on planetary formation. The synergy between the MICADO high-contrast imaging mode and additional techniques like astrometry (GAIA) and radial velocity (VLT/ESPRESSO) will offer a unique view of the planetary system architecture at all orbits

(for the giant planet population). It includes to characterization of their frequency, multiplicity, distribution of mass and orbital parameters (period, eccentricity) for a broad range of stellar properties (mass, metallicity and age). Observables will be directly confronted to predictions of population synthesis models for various types of formation mechanisms (core accretion, gravitational instability or gravo-turbulent fragmentation).

2 What are the initial conditions of planet formation? The high-contrast mode of MICADO combined with the large field of view of the near-infrared camera will offer the unique possibility to explore the properties and morphology of young protoplanetary and debris disks at an unprecedented spatial resolution. Asymmetries (cavity, gap, hole, clump, vortex…) will be actually connected to the various physical processes at play including planetary formation itself. This will allow identifying the key mechanisms of dynamical evolution (planet-disk and planet-planet interactions) of planetary architectures.

3 What are the physical properties of young Jupiters and Saturns? There are still large uncertainties crossing two orders of magnitude to predict basic properties such as the luminosity of young Jupiters and Saturns. We still do not understand how the gaseous component is transferred and accreted from the protoplanetary disk onto the planetary atmosphere. The masses of young imaged exoplanets are currently predicted by non-calibrated evolutionary models. The synergy between the MICADO high-contrast imaging mode and additional techniques will offer the unique possibility to simultaneously derive the dynamical mass together with the orbital properties and the luminosity of the young Jupiters and Saturns. This will set stringent constraints on the phase of planetary atmosphere formation and will offer unprecedented tests for current theoretical predictions of giant planet formation and evolution.

7.2 Importance of MICADO

MICADO is a general purpose instrument and as such will be able to tackle some particular aspects of the general science case described above. For that reason, a high contrast imaging capability is foreseen to take advantage of MICADO pending the installation of a dedicated facility on the E-ELT (EPICS) where the objective will be to address the case of more mature/colder exoplanets (PCS-like). The interest for MICADO in this field is the obvious gain in angular resolution with respect to the current or near term facilities like GPI/SPHERE and JWST. Earlier in this decade, NACO, for instance, has open up a window in exoplanet science. It has been able to detect (Lagrange et al. 2010, Bergfors et al. 2011) and study (Janson 2010, Bonnefoy et al. 2011, Chauvin et al. 2012) young giant exoplanets as well as circumstellar disks (Lagrange et al. 2012a, Boccaletti et al. 2012), but also forming planets buried in protoplanetary disks (Quanz et al. 2013). This has been achieved owing to the use of a) pupil tracking to stabilize the telescope/instruments aberrations with respect to the detector while the field rotates and b) dedicated filters to reduce the star/planet contrast (especially in the L band). The same kind of general purpose instrument on a ~40-m telescope will improve significantly the angular resolution by a factor of 4 to 5, and will contribute to the exoplanets science providing the observing strategy and observing modes are planned to achieve large contrasts around bright stars.

Given the current estimations of performance and limitation, three particular areas were identified as niches for MICADO in the context of planetary systems.

Study of nearby known planetary systems: Assuming MICADO is able to achieve the same level of contrasts as NACO, a beta Pic b-like object becomes easily detectable at ~2 AU instead of 8-10 AU with the capability to extend this minimal distance even closer in (down to 1 AU for a star at 10-20 pc). MICADO will have the capability to reach closer physical separations than NACO and even SPHERE on nearby targets (<50 pc). Since planetary systems are found to be compact in RV surveys (discovery of planets at long periods favours the existence of other planets at shorter periods), it is obviously crucial to reach small separations. In addition, this range of physical distances is overlapping the one probed with RV (Figure), which now starts to be applicable on young early type stars although active (Lagrange et al. 2012b). The GAIA satellite will also bring new detections or limit of detection in the same range of physical distances as probed with MICADO. Therefore, it will become possible to connect these various techniques for the very same systems and derive constraints on the true mass of planets. A more precise calibration of evolutionary models will become feasible hence with the advantage to ultimately perform better spectral characterization (from photometric data or even spectroscopic data). This category of observations will provide information to address the question related to physical properties of exoplanets.

For observing young and nearby stars, MICADO must be capable of pointing bright stars (V>2-3). The most appealing targets will be known beforehand from SPHERE or from RV and astrometric surveys. Because of instrumental constraints these observations will be done in narrow bands to cope with the effect of atmospheric dispersion at the coronagraphic mask plane.

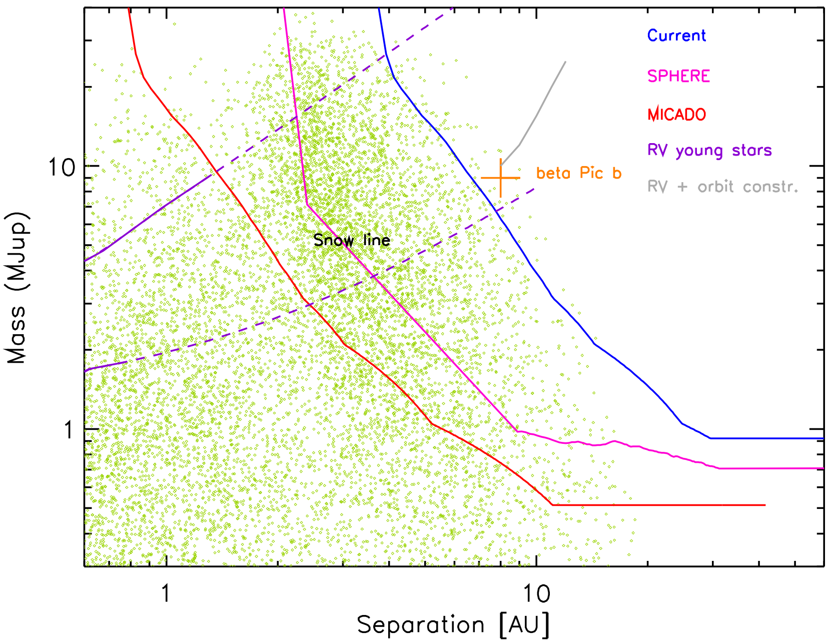

Figure 7.2: *Estimated contrast of several instruments compared to population synthesis (from Mordasini et al. YEAR) assuming a 10Myr young star at 20 pc.*

Planetary systems in young distant associations: A complete new range of targets will be attainable with MICADO given the larger collecting area and the gain in resolution. MICADO will be able to search for young planets in distant (>50-100 pc) young star associations, like for instance the Sco Cen associations that has been fruitful for the search of exoplanets and disks (Bonnefoy et al. 2016; Wagner et al. 2016, Kasper et al. 2015, Wagner et al. 2015, Draper et al. 2016). Typical performance will allow the detection of massive planets (>5 MJ) on wide orbits (>10 AU) complementing the current performance of SPHERE in these young associations. This category of observations will provide information to address the question related to how planet form.

Observations should be preferentially performed in K band with the additional ability to use narrow bands to derive near IR colors and to put constraints on some atmospheric properties like temperature and surface gravity.

Planet-disk interactions: The observation of circumstellar disks is strongly connected to that of exoplanets as the latter form in the former. Here again, with the same contrasts than those achieved with NACO, there are several interests to the imaging of protoplanetary and debris disks with MICADO owing to the gain in angular resolution and sensitivity. There are hundreds of stars known with IR excesses detected from unresolved photometry in the IR (Beichman et al. 2006 for instance). The modelling of their spectral energy distribution informs us about dust properties but the knowledge of the dust spatial distribution is important to remove some degeneracies. SPHERE and GPI have literally boosted disk science by improving contrast. In the first two years of operations, these instruments have provided several important discoveries of new disks (Lagrange et al. 2015, DeBoer et al. 2016, Feldt et al. 2016) or structures in known disks (Benisty et al. 2015, Perrot et al. 2016), both in the protoplanetary regime (the gas dominates the dynamic) or in the debris disk regime (gas is mostly evacuated).

MICADO can potentially resolve some of the disks observed recently by Spitzer and still out of reach from SPHERE or even JWST (because they are too small or too faint). Measuring the size of the disks as well as their surface brightness is the key to determine the location of the planetesimal belts, which are the seeds for planets. In addition, near IR colors are important to measure the scattering efficiency and hence can bring constraints on the dust properties (Debes et al. 2009, for instance).

For disks that are already known from previous observations, the improvement of angular resolution will be valuable to carry out dynamical studies of structures. Any structures (warps, clumps, offsets, spirals) deviating from the simple assumption of an axi-symmetrical system is of interest in the context of planetary formation (see Lee & Chiang et al. 2016). Either some of these structures can be indirectly generated by planets or may lead to planet formation. Here the advantage of MICADO is to resolve angularly these structures with unprecedented details, but also bring time resolution to determine their dynamics. This work has been started with SPHERE (Boccaletti et al. 2015, Figure 7.3) and we anticipate that it will become of great interest with MICADO. This category of observations will provide information to address the question related to the initial conditions.

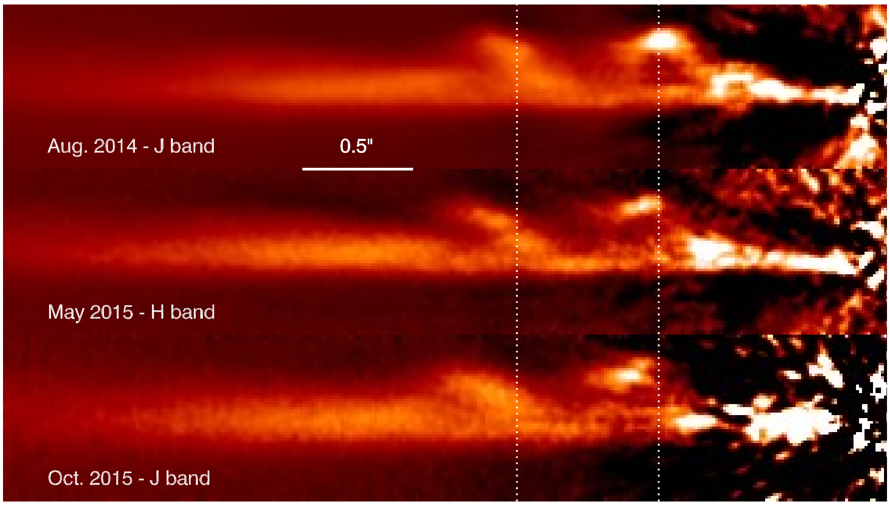

Figure 7.3: *Images of the AU Mic debris disk obtained with SPHERE (Boccaletti et al. in prep.) showing reccurent features moving probably outwards from the system at large speeds.*

References:

8. Solar System Science

There was no reference to this in Phase A – new.
Responsible: Frédéric Merlin, Benoit Carry
Contributors: T. Ercenez, T. Fouchet Technical Templates: A.20, A.21, A.22 (Imaging); A.23, A.24 (Spectroscopy)

The physical properties of solar system objects, as well as their composition, are active studies currently explored through photometric and spectroscopic investigations. These observations have been collected during spacecraft flybys as well as ground-based telescopes. Both these approaches are complementary: spacecraft visits provide extremely accurate compositional and chronological data, while ground based observations allow for systematic surveys, and therefore a global appraisal of the compositional diversity of the planets and small body population as a whole. The last 20 years of ground-based exploration performed in the visible and near infrared allowed tremendous discoveries in different fields, such as the characterization of the physical and chemical properties of the surface of the biggest asteroids, satellites of the Giant planets and those of the biggest and brightest Trans-Neptunian-Objects (TNOs). The monitoring of the small populations reveal transient activity while the observations of the giant planets gave us deeper insights into the temporal and spatial evolution of large atmospheric formations. Such investigations have mainly been limited by the spatial resolution of current ground-based telescopes and thus MICADO will provide an opportunity to significantly develop ground-based studies of solar system objects.

8.1 Outstanding Questions

The exploration of the Giant Planets and minor bodies of the solar system has provided key information about the origin and evolution of the inner and outer Solar system. In the case of all giant planets, the escape velocity is very high (61 km/s in the case of Jupiter) and, because of the low temperature, the Maxwell velocity of the atmospheric molecules is very low. As a result, even the lightest elements (H_2, He) could not escape over the whole history of the Solar system. The giants' atmospheres should thus have retained their proto-solar material, more or less enriched from the contribution of the icy core and should be considered as the most primitive witnesses of the early solar system. Our knowledge has strongly benefited from space missions. From Galileo, we have a good understanding of Jupiter's thermal structure, chemical composition and magnetospheric environment but there is still debate about the nature of the heating source responsible for the high thermospheric temperatures (precipitating particles and/or gravity waves). The cloud structure of Jupiter is globally understood but the nature of the Great Red Spot, a giant anticyclonic storm, colder and higher than its environment, and its internal structure appears to be very complex and needs further investigation at high spatial resolution with MICADO. The Cassini mission, which will end in late 2017, provides deep insights into the saturnian system during a little bit less than half a saturnian year, giving strong but incomplete constraints on the properties of its atmosphere. Quick flybys of Uranus and Neptune by Voyager revealed that the magnetospheres of both planets are highly inclined and offset from their rotational axes, suggesting that they are significantly different from other magnetospheres. Voyager also identified two new rings around Uranus and discovered Neptune's rings, originally thought to be only ring arcs, but they were found to be complete, albeit composed of fine material. Neptune, originally thought to be too cold to support atmospheric disturbances, was found to host large-scale storms (notably the Great Dark Spot). High spatial resolution planetary space missions have already been powerfully complemented by ground-based AO observations. Adaptive optics is particularly well suited for planetary science, since solar system bodies have temporal behavior that requires regular monitoring.

The near Infrared wavelength range give access to spectral features associated with molecules H_3^+, H_2, H_2S, H_2O, CH_4, and hydrocarbons located in the atmosphere or in the rings of the giant planets. Narrow-band filter, infrared observations have provided maps of the emission from the H_2 S1(1) quadrupole line and several H_3^+ lines in Jupiter's auroral zones (Lellouch et al. 2005). Uranus's rings and clouds have been monitored (de Pater et al. 2002). A real temporal variation in the occurrence of Neptune's deep clouds has been detected, pointing to underlying variability in the convective activity at the pressure of the main cloud deck near Neptune's south pole and also in the main observable cloud belt at 30-40°S (Irwin et al. 2016). During the last decade it has been possible to determine the physical properties (spin, size, and shape) of minor bodies in the solar systems, namely asteroids, comets and TNOs, which have preserved chemical, dynamical and chronological information on the formation and evolution of the Solar System.

Disk-resolved imaging is the best method to provide very accurate measures of the size, spin direction, and shape of asteroids (Carry et al. 2012). This research area is also growing quickly, with the development of new methods that combine the different techniques available (see the review by Durech et al. 2015). However, the minor planets studied so far are limited to the main-belt asteroids (with the exception of a few near-Earth asteroids). The angular resolution provided by MICADO/E-ELT will open several other more distant classes of targets to these studies.

Spectroscopic reflectance spectra in the Visible-Near infrared (VNIR) obtained using FORS, SINFONI, ISAAC or Xshooter at the VLT or using the IRTF and CFHT facilities have allowed to characterize the surface of several dozens of objects and classify the population of asteroids into different spectral groups. This scheme mostly relies on the photometric level and the spectral characteristic of the continuum, and in few cases the presence of absorption bands, indicating the properties of the minerals or the chondrites (DeMeo et al. 2015), the physical properties of ices (Merlin et al. 2015) or even revealing aqueous alteration (Hiroi et al. 1996) or space weathering processes (Brunetto et al. 2014) acting on these atmosphere-less bodies. The distribution of spectral types within the main belt is one of the main constraints of the Grand Tack and Nice models. Hence, the asteroids have been moved by giant planets migration. These scenarios also support the presence in the inner solar system of volatile-rich objects that were formed in the outer solar system. Also, we can get clues on radial chemical gradients in the solar nebula. These results need deeper investigations and a more complete temporal monitoring, only accessible from ground-based observations and high spatial abilities, as those offered by MICADO/E-ELT.

8.2 Importance of MICADO

As described above, space missions and ground based observations considerably improved our knowledge of the properties of the solar systems, and hence its formation and evolution. However, the limited spectral resolution of the space instruments, the short duration of these missions compared to the time-scale of the processes being monitored, or the limited spatial resolution from ground-based instruments still leave many unresolved questions. The high spatial resolution of MICADO will offer the possibility to carry out deeper investigations of a large fraction of the bodies in the solar system, including as yet unvisited objects. In detail, MICADO will give us new constraints on the following subjects:

Physical characteristics of minor bodies of the solar system: The study of the physical properties of these small bodies and their multiplicity. The angular resolution provided by MICADO will open several new classes of targets to these studies (see Figure 8.1). For each class, we provide some typical values for the angular diameter, magnitude, colours, and apparent motion. As an example, only 11 over the 24 classes in the asteroid classification have density estimates. As a result, only 12 classes have mineralogical interpretation, which is the ultimate goal to understand the distribution of elements in the primordial nebulae out of which the terrestrial planets formed. For more distant objects, and for the biggest ones, mapping of surface features will possibly provide us a new powerful tool to provide spin vectors and constrain the main chemical compounds distribution on those surfaces.

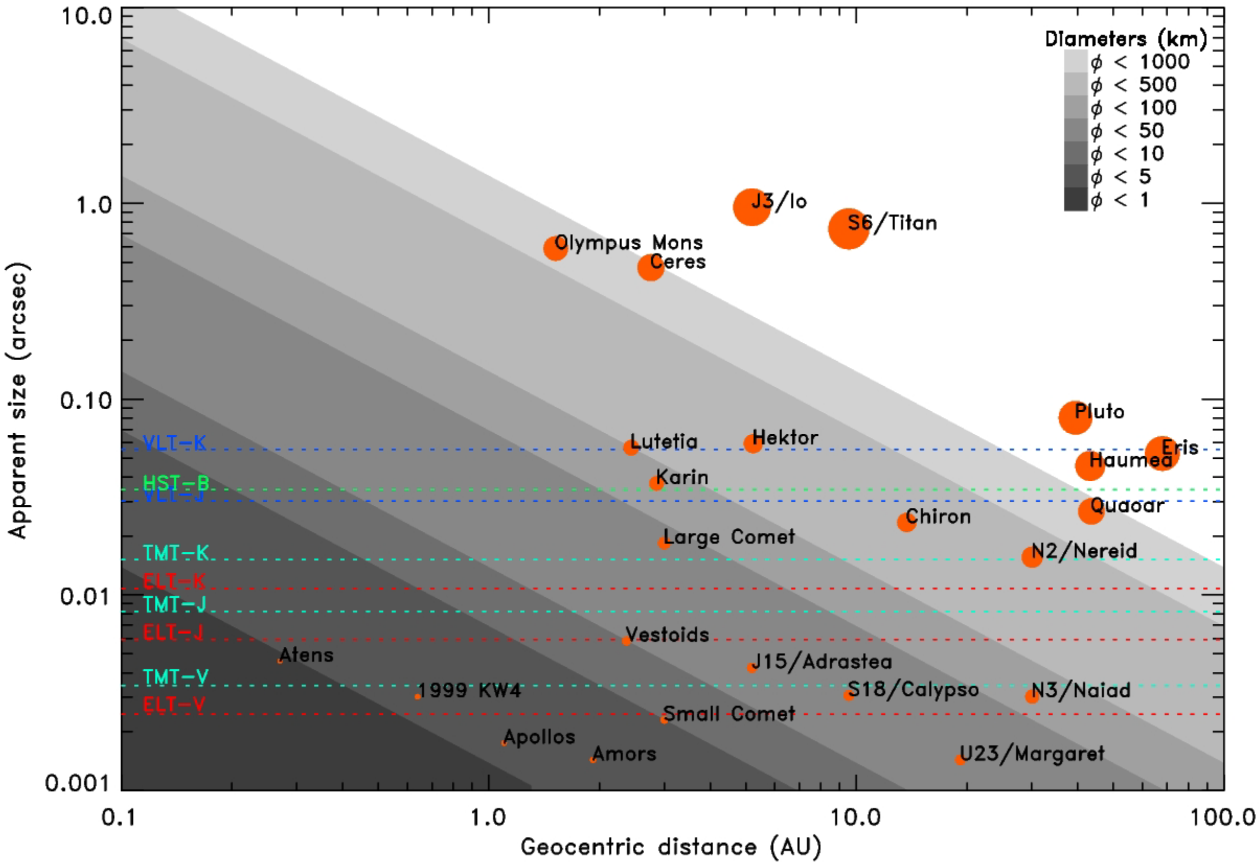

Figure 8.1: *Angular size of minor planets as function of their geocentric distance. The angular resolution limits for the HST, the VLT, the TMT, and the E-ELT are shown, at several wavelengths. MICADO will allow the observation of 1) near-Earth asteroids, currently too small in angular size for either HST or VLT; 2) small main-belt asteroids such as the members of young dynamical families; 3) comet nuclei of average diameter; and 4) the largest trans-neptunian objects.*

Another research area that appeared in the late 1990s (Merline et al. 1999) is the study of the multiplicity of these bodies, thanks to the advent of large telescopes equipped with adaptive-optics (e.g. CFHT, VLT, Keck). From the study of the companion orbit, the mass can be obtained, and once combined with the volume estimate, this yields the bulk density of the minor planet, a key parameter to infer its composition and internal structure (e.g. Carry 2012, Margot et al. 2015). With current technology, we have access to all the main-belt asteroids (orbits between Mars and Jupiter) which physical diameter is above 100km. However, it is of most interest to have access to smaller bodies, such as the members of young dynamical families: e.g. Karin's family, or the Vestoids that are ejecta from Vesta. Indeed, small (few km) targets are affected not only by gravitation but also by non-gravitational effects, such as the Yarkovsky and YORP effects. Studying small families will allow to constraints to be put on the characteristic timescale of these effects, the influence of the shape and interior structure (Scheeres and Gaskell 2008 for instance). . The population of TNOs contains the highest number of multiple systems (with respect to the inner Solar System). However, this statistic is biased as only the largest TNOs have been imaged (see Noll et al. 2008 for more information on TNO binaries). The imaging capabilities of MICADO will allow the search for companions around faintest targets, hence bodies with smaller physical diameters.

The surfaces of the TNOs are coated with ices, but we have very little knowledge on their physical properties. However, the largest objects have an angular diameter that can be resolved by MICADO. Combined with the knowledge of their mass (from the study of satellites' orbit), density estimates will be possible. For instance, the large TNO (136108) Haumea, which surface is composed almost of pure water ice, has a density estimated between 2.6 and 3.6 g/cc, far above the water ice density. But its volume has only been estimated through indirect methods (e.g. Raboniwitz et al. 2006). Direct imaging of its apparent disk will yield precise volume, hence density and ultimately constraints on its internal structure (presence of a dry silicate core). Contrary to asteroids, almost fully homogeneous, several TNOs and Centaurs show clear surface heterogeneity (e.g. Merlin et al. 2005). High signal to noise level of spatially resolved images at different particular wavelengths could be used advantageously to clearly confirm the heterogeneity of such bodies, as well as retrieve valuable information of the chemical composition, when accurate spectroscopy is not available due to the faintness of these objects (Trujillo et al. 2011).

Near-Earth Asteroids are asteroids with orbits that cross those of the 4 telluric planets. They compose a short-lived population suffering close encounter with planets, including the Earth. Given their small physical size, they are much more sensitive to the non-gravitational effects such as YORP and Yarkovsky. Their heliocentric distances also make them sensitive to some relativistic effects (Mouret et al. 2010), hence the knowledge of their physical properties (spin, size, and shape) is required to discriminate between the relativistic and non-gravitational effects on their orbital evolution. The nucleus of comets remains very elusive to us, with only a handful imaged by spacecraft.

The possibility to image comet nuclei with MICADO would allow a measurement of the amount of ejected material (gas and dust) in coma observations. This is a unique opportunity to finally calibrate the comets internal structure models, and mass production rates. The study of the spin evolution with the gas ejection will also allow the study of the influence of non-gravitational effects on the comets nuclei.

Imaging the surface of the smallest bodies of the solar system: The surface of minor bodies, such as asteroids or TNOs, are coated with silicates, minerals or ices, which display many absorption bands in the near-infrared wavelength range (e.g: Barucci et al 2008). A key question is for instance the distribution of water ice in the Solar System, as it has been detected only on the largest bodies, but this may be an observational bias. The faint apparent magnitude of the Centaurs, Trojans and TNOs do not allow sufficient S/N observations, with the exception of the few largest, to be able to investigate their properties. MICADO will change this. A combination of narrow band filters and, even better, low resolution (R~1000 - 5000) slit spectroscopy, will allow the identification of chemical compounds and their properties (dilution level, phase) on the surface of the smallest tail of asteroids and the medium-sized class of TNOs and Centaurs. This will allow us to study the relative abundance of minor compounds, which could be primordial or formed by space weathering processes. Indeed, the analyses of the effects of the radiation and possible internal processes will be also possible, by the search and detection of crystalline or amorphous water ice for instance. Retrieving chemical information of the surface of comet nuclei is a difficult task since the surface of comets is mainly depleted of ices, which sublimated at near heliocentric distances. The Deep Impact mission, for instance, has revealed only a few small spots composed of water ice close to the dimly illuminated and cold pole of Tempel 1 at a heliocentric distance of 1.5 A.U. (Sunshine et al. 2006). MICADO will provide the possibility to observe the surface of these objects.

The Trans-neptunian region is still very little known, and the more we learn about TNOs, the more complicated the picture appears. As more objects are discovered, the dynamical theories of the formation and evolution of the solar system must be revised. Large surveys are required to obtain comprehensive information on a range of different object types. MICADO (and ALMA) can be used to go beyond the current limits of terrestrial observations. Satellites such as Spitzer or Herschel have been widely used to contain the physical properties of these uncommon objects (Lellouch et al. 2013). But results are still limited to the biggest and relative dark objects (usually the warmest for IR detection). The study of a population related to TNOs –Centaurs, but also comets, irregular satellites of giant planets or Trojans– should also lead to better constraints on the models of our planetary system.

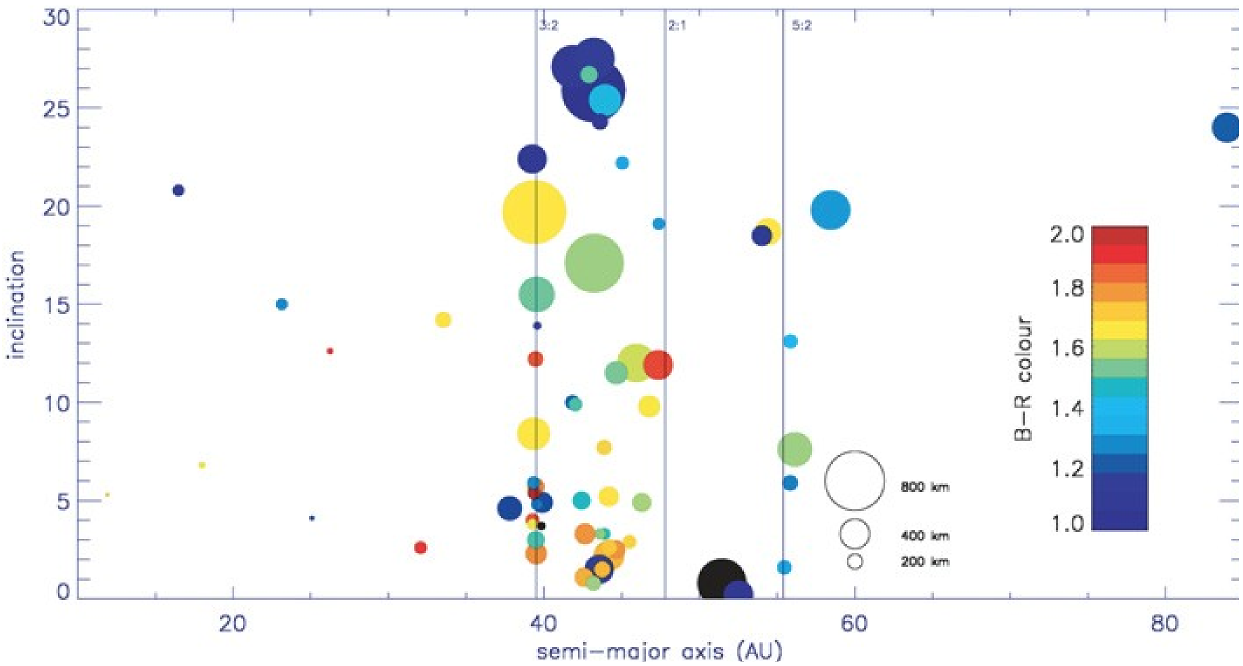

Figure 8.2. *The colours of Centaurs and TNOs (from Doressoundiram et al. 2005), in the inclination vs. semi-major axis plane. Symbols sizes are proportional to the estimated object sizes. The color range has been adopted to scale the objects colour from red (in dark red with B-R=2.0) to blue (in dark blue with B-R=1.0). Three resonances with Neptune are also plotted as vertical lines.*

Colours are the primary property that can be obtained, from broadband photometric observations. The most striking result is that TNOs and Centaurs display a wide range of colors, as can be seen in Figure 8.2, and a size-inclination trend is detected in the TNO population. In particular, Classical objects are bluer and larger at high inclination. Some correlation has been found with orbital parameters: cold Kuiper Belt objects are rather red, while hot Kuiper Belt objects are display the whole range of colors (Doressoundiram et al. 2002; Gulbis et al. 2006). This supports the idea that these two populations have different origins. Several groups observed that objects with perihelion distances greater than 40 AU display redder colors (Tegler & Romanishin 2000; Boehnhardt et al. 2002; Doressoundiram et al. 2003). A taxonomy has been developed (Barucci et al. 2005; Fulchignoni et al. 2008): the different colours might represent different evolutionary states of the surface. The reddest visible spectra also flatten toward the near-infrared, which is consistent with the idea that TNOs and Centaurs surfaces are made of an irradiated crust. The different colours should therefore be interpreted as a result of the competition between several processes: 1) Composition: since TNOs have formed in different locations, different compositions should be inferred. Alteration of different ices might produce different compounds with different properties. 2) Irradiation: laboratory experiments showed that irradiated ices become redder with increasing irradiation. Indeed, molecules progressively loose their hydrogen atoms, which results in a polymerization of the surface layer, and the formation of a crust (Strazzula & Palumbo 1998). 3) Collisions: their main effect is the exposition of underlying non-irradiated material to the surface. 4) Internal processes: comet-like activity or cryovolcanism act in the same way than collisions by re-depositing fresh “blue” material on the surface. The activation of such processes depends on the distance from the Sun, and the size of the object, but also on the thickness of the crust on the surface. Comet-like activity has been observed at large heliocentric distances, and has even been supposed for TNOs (Hainaut et al. 2000). Some Centaurs like Chiron (Meech & Belton 1990) or Echeclus (Rousselot 2008) display cometary activity. MICADO will provide such information for a larger fraction of the whole population and will strongly constrain the importance and rôle of each process.

Beyond photometric observations, the ideal method to further investigate the surface composition of TNOs and Centaurs remains spectroscopy. To interpret the features that could potentially be present on the spectra, radiative transfer models have been developed, using either the Hapke theory (Hapke 1981) or the Shkuratov et al. (1999) method. However, the results given by spectral modeling are only indicative. A quantitative interpretation is impossible without additional knowledge of the albedo, and different mixtures (geographical, intimate or molecular)~~,~~ using different compounds, different grain sizes, or different temperatures. In spite of the numerous dependences of the model, some interpretation can be made, and various ices have been detected on surfaces, as well as silicates and solid organics. Water ice should be the main component of TNOs and Centaurs, and many objects do show the water ice feature at 1.5 and 2.2 μm in their spectra. The debate is still open as to whether water ice was amorphous or crystalline in the proto-solar nebula. All spectra with signal to noise high enough show the presence of the crystalline water ice feature at 1.65 μm, which implies at least partial crystallinity of original the ices. Nonetheless, when trying to model the spectra, the best fit model is usually obtained when including a small amount of amorphous water ice (Merlin et al. 2007). The issue is that if the water ice was amorphous, then it could survive for the age of the solar system on these objects due to the very low temperature of the trans-neptunian region. We can therefore conclude that either the ice was crystalline at the beginning, or that amorphous ice has been heated, leading to the phase transition from amorphous to crystalline water ice. However, back-amorphization is expected to occur in less than 10^{7-8} years (Cooper et al. 2003). The presence of crystalline water ice therefore suggests a recent resurfacing event, that may be due to collisions, or internal activity. The detection of ammonia –which should also be depleted rapidly from any surface– on Charon (Cook et al. 2007) and possibly also Orcus also raises question on the internal activity of such objects. Water ice is detected on large objects as well as on the smallest ones (Typhon for example, Guilbert et al. 2009). From both theoretical assumptions (McKinnon et al. 2008) and observations (Guilbert et al. 2009), a size limit has been determined to the systematic detection of water ice on the spectra: objects with diameter bigger than 680km should display water ice features, while smaller objects spectra could present or not these features. We have great expectations for dramatic developments in this area using MICADO.

Spectroscopy of icy satellites and dwarf planets: In addition to resolved imaging of the surfaces of small bodies, discovering new multiple systems and constraining their orbits and internal bulk densities, spectroscopy is the best tool to investigate the surface properties, as well as those of the atmosphere (e.g. Merlin et al. 2010 with SINFONI or Protopapa et al. 2008 with NACO for the surfaces of the Pluto-Charon couple). MICADO, will provide us enough spatial and spectral resolution to discover minor species and follow the possible temporal variations. The combination of knowledge on the physical and chemical properties of the surfaces with constraints on the bulk density of these objects is necessary to fully constrain their internal structure.

Most of the satellites of the Giant planets are barely resolved with ground-based observations, however some have been visited by spacecraft (Voyager, Galileo, Cassini). The resolved images from these spacecraft are taken over a limited time span, and several satellites exhibit clear temporal evolution. The explanation for the physical and chemical processes observed require continuous monitoring for Titan (Hirtzig et al. 2007) or Enceladus (Porco et al. 2006) as two examples. Earth-based instruments, with lower spatial resolution than spacecraft, but with time coverage flexibility, are a necessary complement for the space missions. With the capabilities of MICADO (imaging and spectroscopy), it will be possible to investigate the activity of the heavily " geologically modified" satellites (Johnson et al. 1998). This requires the coupling of good spatial resolution (a few kilometers/pixel for the satellites of Jupiter) and good spectral resolution (R~1000 to 10000) to allow us to study the detailed physical and chemical processes acting on the most active satellites and the biggest dwarf planets, where recent observations suggest the presence of jets or transient atmosphere (Küppers et al. 2014, Sicardy et al. 2005). The capabilities of MICADO will allow us to map and accurately constrain the chemical compounds detected on several objects such as: 1) the SO_2 distribution on the surface (absorption bands of SO_2 ice, Laver and Pater 2008) and in the atmosphere of Io (from electron impact induced fluorescence spectrum of SO_2 for instance, Ajello et al. 2008), to conclusively determine the relative importance of these frost deposits in sustaining the local and global atmosphere and investigate the mechanisms in action in Io's atmosphere (Moullet et al. 2010). 2) The ice and salt distributions on the surface of Europa, which is in addition a major exobiological target with its possible sub-surface briny ocean buried under a water-ice dominated crust of several km-thick. High spectral resolution (0.5 nm) is required to detect narrow signatures in the wavelength range 1.45-2.45µm. Depending on the hemisphere, the spectra are globally dominated by crystalline water-ice distorted and asymmetric absorption features, or dominated by sulfuric acid hydrate (Carlson et al. 1999) coming from Io-genic sulfur ion bombardment. 3) CH_4, N_2 and hydrocarbons in the atmosphere of Titan. Titan is the only satellite with a dense atmosphere, which is primarily made of nitrogen and methane. It harbours an intricate photochemistry, that populates the atmosphere with aerosols, but that should irreversibly deplete the methane. The observation that methane is not depleted has motivated the further study of Titan's methane cycle. The features that found in Titan's atmosphere can last for timescales varying from years to days. For instance, the reversal of the north–south asymmetry is linked to a 16-year seasonal cycle. Diurnal phenomena have also been observed, like a stratospheric haze enhancement or a possible tropospheric drizzle. All these observations need high spatial capabilities and long term monitoring. Initial data from VLT/NACO (see Figure 8.3) show the potential of MICADO.

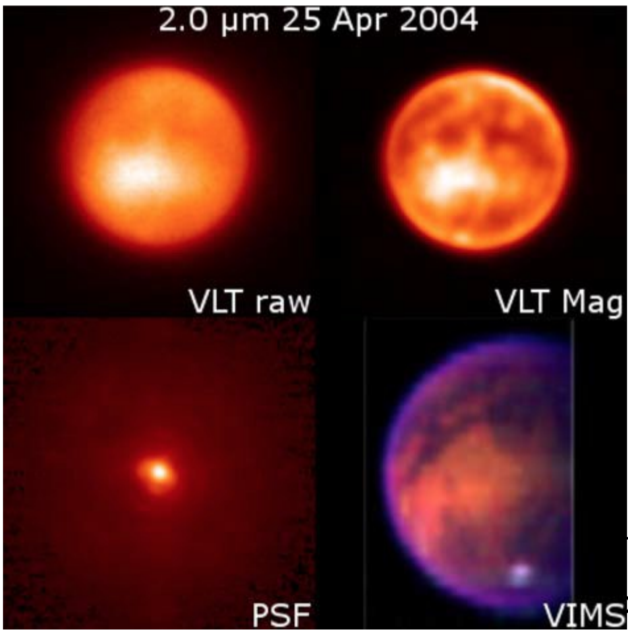

Figure 8.3: *An example of the deconvolution of small bodies imaging. On the upper left corner is a "raw" VLT/NACO image acquired on 25 April 2004 at 2.0µm of Titan. On the lower left corner is the point-spread function (PSF) showing the diffraction phenomenon that were not possible to correct with the adaptive optics. On the upper right corner is the result of the Magain deconvolution. In the lower right corner an image from the spacecraft Cassini and its instrument VIMS can be considered as a "true/unmodified image". This proves that all the features, barely visible on the "raw" image, but seen in the deconvolved image, are real. From Hirtzig et al. (2009). Better spatial resolution, such as that from MICADO/E-ELT,*

coupled with deconvolution image processes show the capability to reach the level of accuracy provided during close encounter missions.

4) The H_2O, CO, CH_4, N_2 distribution on the surface or in the atmosphere of Triton. Ground-based observations provided the first detection of CO in Triton's atmosphere, and the first observation of CH_4 gas since Voyager (Lellouch et al. 2010). Results indicated (i) a CO/N_2 atmospheric abundance consistent with its surface abundance (0.05 %) (ii) a CH_4 column several times larger than measured by Voyager in 1989. Possible interpretations of the CO abundance are that (a) CO is diluted in N_2 ice and its atmospheric abundance is enhanced by the "detailed balancing" effect or that (b) it results from localized CO-rich patches. Although the first hypothesis is thermodynamically more plausible, it has not been confirmed observationally. For methane, the increase since Voyager is best explained if Triton's surface temperature increased from the 38 K value measured in 1989, but once again, measurements are lacking. Without spatially resolved observations, conclusions as to the origin of these changes remain uncertain and MICADO is needed to make progress. MICADO will also make it possible to extend this kind of analysis to the other medium-size satellites and dwarf planets (such as Makemake, and Eris), and allow us to consider the role of other parameters on the evolution of these bodies, such as the heliocentric distance (i.e: the temperature, past and ambient conditions), the local environment (i.e: effect of the planets for the satellites), and the physical properties of the different objects (size, chemical composition).

The composition and temporal variation of the atmospheres of giant planets: The larger angular sizes of Jupiter and Saturn allow studies of atmospheric dynamics on these planets in far greater detail than on Uranus and Neptune. For example, the MICADO pixel scale would be 20, 40, 80, and 120 km at the sub-observer point for Jupiter, Saturn, Uranus, and Neptune, respectively. Reflectivity observations that make use of the variable opacity of methane and center to limb variations will enable altitude determinations of the cloud features in storms and vortices, 1-2.5 µm mapping of H_2O-ice and hydrocarbons distributions (Baines et al. 2009) could clarify their origins and dynamics, and repeat observations will explore the motions and evolution of these phenomena. Among the phenomena of interest are variable Jupiter's South Equatorial Belt and North Temperate Belt Disturbances (Sanchez-Lavega et al. 2008), Saturn's recurrent Great White Spots (Sanchez-Lavega et al. 2011, Sayanagi et al. 2013), and the ongoing evolution of Jupiter's Great Red Spot as it diminishes in size. MICADO observations will also assist investigations of atmospheric evolution on these dynamic worlds as the events unfold.

Since its discovery in Jupiter's polar regions at 2 µm in its $2\nu_2$ band (Drossart *et al*. 1989), the H_3^+ ion has been the subject of considerable interest and recognized to be an important tracer of the Jovian upper atmosphere and the coupling with Jupiter's magnetosphere, and more generally a tracer of Giant Planet upper atmosphere energetics and dynamics (see review by S. Miller *et al*. 2006). Studies have been conducted to determine the mean H_3^+ line emission intensities, column density and temperatures (kinetic, rotational and vibrational) in the northern and southern auroral regions, so as to infer its role in the auroral atmosphere heat budget. Analyses have been also made to characterize the morphology and variability of the auroral emissions and measuring the non-auroral (mid-to-low latitude) emission, and evaluate the large-scale circulation at sub-microbar levels. Separating the temperature and column density parameters in existing observations has turned out to be difficult. High-spectral-resolution spectral-imaging observations of H_2 and H_3^+ in the 2 µm region in both hemispheres provide information on the composition, temperature and potentially wind speeds, in the Jovian auroral upper atmosphere. Results on the H_2 and H_3^+ emission spatial distribution show clear morphological differences between both poles with large spatial contrasts (see Figure 8.4). With the exception of the hot spot near 70° north, longitude 155°, Lellouch et al. (2006) find that the H_3^+ column density is the main parameter driving line emission variations. The general constancy of H_3^+ temperatures over the northern auroral region is probably related to the fact that H_3^+ is the main cooling agent at sub-microbar levels, owing to its excellent radiative properties and despite its small abundance (Miller et al. 2000). The rapid variation of the H_3^+ cooling rate with temperature ensures that large variations of input energy will result in only modest temperature variations. In contrast, the northern hot spot, which is prominent at a variety of other wavelengths, exhibits a Temperature about 250 K higher than other regions. A partial explanation might invoke a homopause elevation in this region, leading to a local increase in the methane abundance and an associated decrease in the contribution of the deeper and colder H_3^+ component. However, this scenario raises a number of unsolved questions; more generally, the different H_2 and H_3^+ distributions remain difficult to explain (Raynaud et al. 2004). At Saturn, studies of the influence of the rings upon the H_3^+ distribution is a possible objective, such as the identification and evolution of large scale structures, such as "great white spots" and the main seasonal evolution of its upper atmosphere.

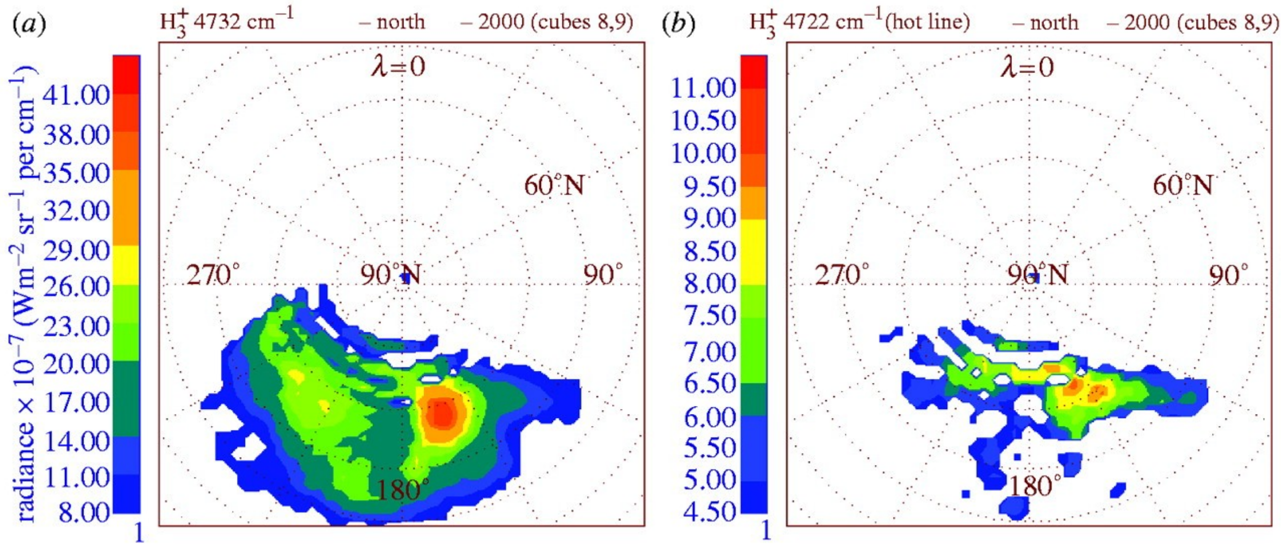

Figure 8.4: *Projected radiance maps in the (a) H_3^+ 4732.0cm−1 $2v_2^2$ R(7,7) line and (b) H_3^+ hot band 4721.8 cm−1 $3v_2^2$-v_2R(6,7) line. Latitude and System III longitude grids are indicated. Note the different colour scales for each plot. The noise level is about 4×10−7Wm−2sr−1 per cm−1. From Lellouch et al. 2006*

Because Uranus and Neptune are far out from the Sun, in a less dense part of the proto-planetary disk, the accretion processes of the rock and ices of the central core probably took more than for Jupiter and Saturn. Jupiter and Saturn probably accreted in 1 to 3 Myr, while Uranus and Neptune may have taken about ten times longer (Taylor, 1992). The accretion phase of the surrounding nebula may then have taken place at a time when the primordial gas had been already partly swept away in the T-Tauri phase of the young Sun, and thus less primordial gas may have been available. This scenario could explain why Uranus_and Neptune have a very large fraction of their mass in their central core. But it remains unclear why Uranus and Neptune so different from each other. In spite of their established status as "icy giants", and their similarities in global atmospheric composition and tropospheric temperature structure, they differ from each other in many ways. First Neptune has an internal source of energy, while none has been detected on Uranus. Second, Neptune has a very efficient dynamical circulation, while Uranus has none. To account for these differences, it has been suggested that both planets might have different internal structures. In Neptune, the heat (originating from the cooling of the planet since its formation) is transported from the interior by convection. Uranus, being closer to the Sun, receives more solar flux than Neptune, which already hampers the escape of internal heat. In addition, the interior of Uranus might have a different stratification, so that convection might be inhibited, which would prevent the upward transport of internal energy. This hypothesis however remains to be tested.

In the near infrared, one of the key studies will be investigation of the composition and vertical structure of these planets' upper tropospheres. In this wavelength regime, the sensing depth for Uranus and Neptune is dependent primarily on the opacity of methane, which varies over several orders of magnitude and thus allows observations to probe to a variety of altitudes. Multi-wavelength and center-to-limb observations will be able to locate and characterize the cloud layers from which incident sunlight is reflected: the uppermost (CH_4) cloud layer, and if it is optically thin enough the (presumably H_2S) cloud below it. Investigations of the CH_4 in the stratosphere will also reveal whether its distribution varies with latitude as well, and will help assess the very different disk-averaged CH_4 profiles Lellouch et al. (2015). MICADO, with its high spatial resolution will provide more insight in the spatial and seasonal variabilitie of CH_4 profiles. Other scientific opportunities with Uranus and Neptune are numerous, and include tracking of cloud features to determine zonal wind speeds. Such an investigation is best implemented with near-infrared imagery over timescales of 2-3 times the planet's rotational period (~30-50 hours).

References:

Ajello et al. 2008, in JGR, 113, E03002. Baines et al. 2009, in Planetary and Space Science 57, Issue 14-15, pp1650-1658. Baines & Hammel, 1994, in Icarus 109, p20. Barucci et al., 2005, in AJ 130, p1291. Barucci et al. 2008, in Solar System Beyond Neptune, p143. Boehnhardt et al., 2002, in A&A 395, p297. Brown and Hand, in the AJ 145, Issue 4, article id. 110. Brunetto et al. 2014, in Icarus 237, pp278-292. Carlson et al. 1999, in Science 286, 5437, pp97-99. Carlson et al. 2005, in Icarus 177, Issue 2, pp461-471. Carry et al. 2010, in A&A 523, idA94. Carry et al. 2012, in P&SS 66. Carry 2012, in P&SS 73. Cook et al., 2007, in ApJ 663, 1406, p1419. Cooper et al., 2003, in EM&P, 92, p261. DeMeo et al. 2015, in Asteroids IV pp13-41. de Pater et al. 2002, in Icarus 160, issue 2, pp359-374. Doressoundiram et al., 2002, in AJ 124, p2279. Doressoundiram et al., 2003, in EM&P 92, p131. Doressoundiram et al., 2005, in Icarus 174, p90. Doressoundiram et al., 2008, in The Solar System Beyond Neptune (Univ. Arizona Press), p91. Drossart et al. 1989, in Nature 340, pp539–541.Durech et al. 2015, in Astteroids IV, p183. Fulchignoni et al., 2008, in The Solar System Beyond Neptune (Univ. Arizona Press), p181. Guilbert et al. 2009, in Icarus 201, Issue 1, pp272-283. Gulbis et al., 2006, in Icarus 183, p168. Hainaut et al., 2000, in A&A 356, p1076. Hanley et al. JGR Planets 119, Issue 11, pp2370-2377. Hapke 1981, in J. Geophys. Res. 86, p1019. Hiroi et al. 1996, in Icarus 119, pp202-208. Hirtzig et al. 2007, in JGR 112, E02S91. Hirtzig et al. 2009, in the A&A Review 17, Issue 2, pp105-147. Irwin et al. 2016, in Icarus 271, pp418-437. Johnson et al. 1998, in Solar System Ices, p511. Kaasalainen et al. 2001, in Icarus 153, p37. Karkoschka, 2015 in Icarus 250, pp294-307. Karkoschka & Tomasko, 2011, in Icarus 211, p780. Küppers et al. 2014 in Nature 505, Issue 7484, pp525-527. Laver and Pater 2008, in Icarus 195, p752. Lellouch et al. 2006, in Phil. Trans. R. Soc. A 364, pp3139–3146. Lellouch et al. 2010, in A&A 512, L8. Lellouch et al. 2013, in A&A 557, A60. Lellouch et al. 2015, in Icarus 253, pp99-114. Margot et al. 2015 in Asteroids IV, p355. McKinnon et al., 2008, in The Solar System Beyond Neptune (Univ. Arizona Press), p213. Meech & Belton, 1990, in AJ 100, p1323. Merlin et al. 2005, in A&A 444, p977. Merlin et al., 2007, in A&A 466, p1185. Merlin et al. 2010 in Icarus 210, Issue 2, p930. Merlin et al. 2015 in A&A 582, idA39. Merline et al. 1999, in Nature 401, p565. Merline et al. 2002, in Asteroids III, p289. Miller et al., 2000, in Phil. Trans. R. Soc. A 358, pp2485–2502 Miller et al., 2006, in Phil. Trans. R. Soc. A 364, pp3121–3137. Millis and Dunham, 1989, in Asteroids II, p148. Moullet et al. 2010, in Icarus 208, p353. Mouret et al. 2010, MNRAS. Noll et al. 2008, in Solar System Beyond Neptune, p345. Ostro et al. 2002, in Asteroids III, p151. Porco et al. 2006, Science 311, p1393. Protopapa et al. 2008, in A&A 490, pp365-375. Quirico and Schmitt, 1997, in Icarus 128, pp181-188. Raboniwitz et al. 2006, in AJ 639, p1238. Raynaud et al., 2004, in Icarus 171, pp133–152.Rousselot 2008, in A&A, 480, p543. Sanchez-Lavega et al. 2008, in Nature 451, Issue 7181, p1022. Sanchez-Lavega et al. 2011, in Nature 475, Issue 7354, pp71-74. Sayanagi et al. 2013, in Icarus 223, pp460-478. Scheeres and Gaskell 2008, in Icarus 198, p125. Shkuratov et al., 1999, in Icarus 137, p235. Slivan et al. 2003, in Icarus 162, p285. Sicardy et al. 2005 in Astronomical Society of the Pacific, ISBN 1-58381-189-3., p908. Sromovsky et al. 2014, in Icarus 238, p137. Strazzula & Palumbo, 1998, in Plan. Sp. Sci., 46, p1339. Sunshine et al. 2006, in Science 311, 5766, p1453. Tegler & Romanishin, 2000, in Nature 407, p979. Trujillo et al. 2011, in ApJ 730, id 105. Tryka, et al. 1994, in Icarus 112, p513

9. High Time Resolution Astronomy

[this needs a proper science case around it – perhaps a stellar section?]

The science that can be addressed use fast time resolving detectors includes:

- Emission processes associated with compact objects – neutron stars, white dwarfs and black holes;
- Stochastic behaviour in accretion disks around white dwarfs, neutron stars and black holes;
- Stochastic behaviour in pulsar magnetospheres – optical/IR counterparts to rotating radio transients and giant radio pulses;
- Follow-up observations of gamma (and other) ray burst transients;
- Time resolved IR observations of magnetars – Anomalous X-ray Puslars and Soft Gamma Repeaters.

These phenomena are examples of extreme physics mentioned in the road map for European Astronomy, although they do not represent by far an exhaustive list. These objects can be studied in the optical, where most current HTRA observations are made, and in the future in the infrared. In the context of the E-ELT, HTRA observations in the near-infrared over the wavelength range 0.8-2μm would make a significant impact on all of these science areas [1,2]. For example in pulsar magnetosphere studies, it is in the near-IR that we expect to see evidence of synchrotron self absorption, which will severely constrain the local magnetic field around the emission zone. The E-ELT would be expected to be able to observe most of the Fermi gamma-ray pulsars – increasing the number of detections from 5, a curiosity, to more than forty, the start of a survey. Time resolved observations are vital to these studies as, for example, time averaged fluxes give misleading estimates of even the luminosity for time varying objects [4]. For more science details see the two Opticon funded publications references 3 and 5.

In summary, a high time resolution capability is a worthwhile option exploring during MICADO's Phase B for both scientific and technological reasons: (i) this would provide an additional unique capability that is not foreseen for any other ELT; (ii) it might be possible to incorporate such a device with very little impact on the overall design of the arm since to a large extent all that is needed is a movable pickoff mirror and an appropriate detector.

References

1. Shearer A., et al., 2008, Proc. SPIE, 6986, High time resolution astrophysics and ELTs: Which wavelength?

2. Shearer A., et al., 2008, in High Time Resolution Astrophysics: The Universe at Sub-Second Timescales, 984, 232, High Time Resolution Astrophysics and Extremely Large Telescopes

3. Phelan et al., 2008, in High Time Resolution Astrophysics: The Universe at Sub-Second Timescales, AIP Conf. Proc. 984

4. Shearer, Andrew, 2008, Astrophysics and Space Science Library, 351, 4020, High Time Resolution Astrophysics and Pulsars

5. Phelan, Don, Ryan, Oliver, and Shearer, Andrew, 2008, Astrophysics and Space Science Library, 351, High Time Resolution Astrophysics

10. Appendix A: Technical Templates

Here all the technical templates will be attached, potentially as a separate document.

End of document